Retrofitting Unreinforced Concrete Masonry to Resist Tornado Loading

by

Evan G. Dorshorst
B.S., Civil Engineering
Washington University in St. Louis, 2012

Submitted to the Department of Civil and Environmental Engineering in Partial Fulfillment of the Requirements for the Degree of

MASTER OF ENGINEERING IN CIVIL AND ENVIRONMENTAL ENGINEERING
at the
MASSACHUSETTS INSTITUTE OF TECHNOLOGY

JUNE 2013

Signature of Author: _____
Department of Civil and Environmental Engineering
May 10, 2013

Certified by: _____
Jerome J. Connor
Professor of Civil and Environmental Engineering
Thesis Supervisor

Certified by: _____
Rory Clune
Massachusetts Institute of Technology
Thesis Reader

Accepted by: _____
Heidi M. Nepf
Chair, Department Committee for Graduate Students

Retrofitting Unreinforced Concrete Masonry to Resist Tornado Loading

by

Evan Dorshorst

Submitted to the Department of Civil and Environmental Engineering on May 10, 2013 in Partial Fulfillment of the Requirements for the Degree of Master of Engineering in Civil and Environmental Engineering

Abstract

Advances in structural design and building materials have significantly increased the performance of many structures under the extreme loading conditions associated with natural disasters such as earthquakes. However, catastrophic structural failure after extreme wind events and tornadoes remains a problem which costs the insurance industry billions of dollars and results in an average loss of 200 lives per year in the United States. Accountable for many of these structural failures, buildings with walls of Unreinforced Masonry (URM) are incapable of withstanding the magnitude of forces brought on by a tornado, and the cracking or failure of just one wall can lead to the progressive collapse of the entire structure. The need to reinforce these systems is large, but retrofitting with conventional steel reinforcement is time consuming and costly; however, externally bonded Fiber Reinforced Polymer (FRP) composites represent a high strength, low cost alternative which and can be installed in a fraction of the time. This thesis investigates the use of FRPs to strengthen URM walls against both out-of-plane flexural loads and debris impact, and attempts to determine if enough strength can be added for such wall assemblies to meet the requirements of a Tornado Safe Room as dictated by FEMA. By adapting current design guidelines and extrapolating evidence on the performance of URM walls strengthened with FRP, a design guide is created which provides the tool necessary to use this innovative retrofitting technique to strengthen URM walls to satisfy both the flexural and impact resistance strength requirements for FEMA Tornado Safe Rooms.

Keywords: Fiber Reinforced Polymer, Masonry, Storm Shelter, Tornado

Thesis Supervisor: Jerome J. Connor
Title: Professor of Civil and Environmental Engineering

Thesis Reader: Rory Clune
Massachusetts Institute of Technology

Acknowledgements

My efforts on this project were only sustained because of the efforts of several others who worked to ensure my successful completion of this project. I would like to express my gratitude to my supervisor Professor Jerome Connor for his guidance and devotion to the advancement of the structural engineering field. Furthermore I would like to thank Rory Clune who provided me with the motivation, support, and guidance necessary to complete this project. I also dedicate this thesis to my parents who have given me many opportunities to challenge myself, expand my knowledge, and receive a world class education.

Table of Contents

List of Figures

List of Tables

Chapter 1 Introduction

Over the past few decades, technological and scientific advancements have led to the development of truly remarkable construction materials such as high strength concrete and steel and a vast array of different structural composites. Structural engineers have utilized these materials allowing for the construction of safer and more innovative buildings. One topical subject of research in the field of structural engineering focuses on optimizing the design of buildings subject to seismic events. Findings from such research allow engineers to design a structure that can provide not only life safety during an earthquake, but can be fully functional and immediately occupied following such an event, with little to no structural damage occurring. These advancements in construction and engineering have revolutionized motion based design, and this focus on seismic design in the United States has no doubt saved thousands of lives and billions of dollars; however, the structural engineering community has failed to address a concern which poses an equally significant threat to our nation's infrastructure, causes significant structural failure, and claims hundreds of lives every year.

Though neglected by many of the country's best structural engineering programs, tornados were responsible for more deaths in 2012 than deaths from U.S. earthquakes in the last 20 years (USGS 2013). According to the NOAA's Storm Prediction Center, the United States experienced 939 earthquakes in 2012, 22 of which proved lethal taking 70 lives. Compare this to data provided by the United States Geological Survey, which indicates that between 1993 and 2003, this country experienced only four deadly seismic events resulting in the loss of 65 lives.

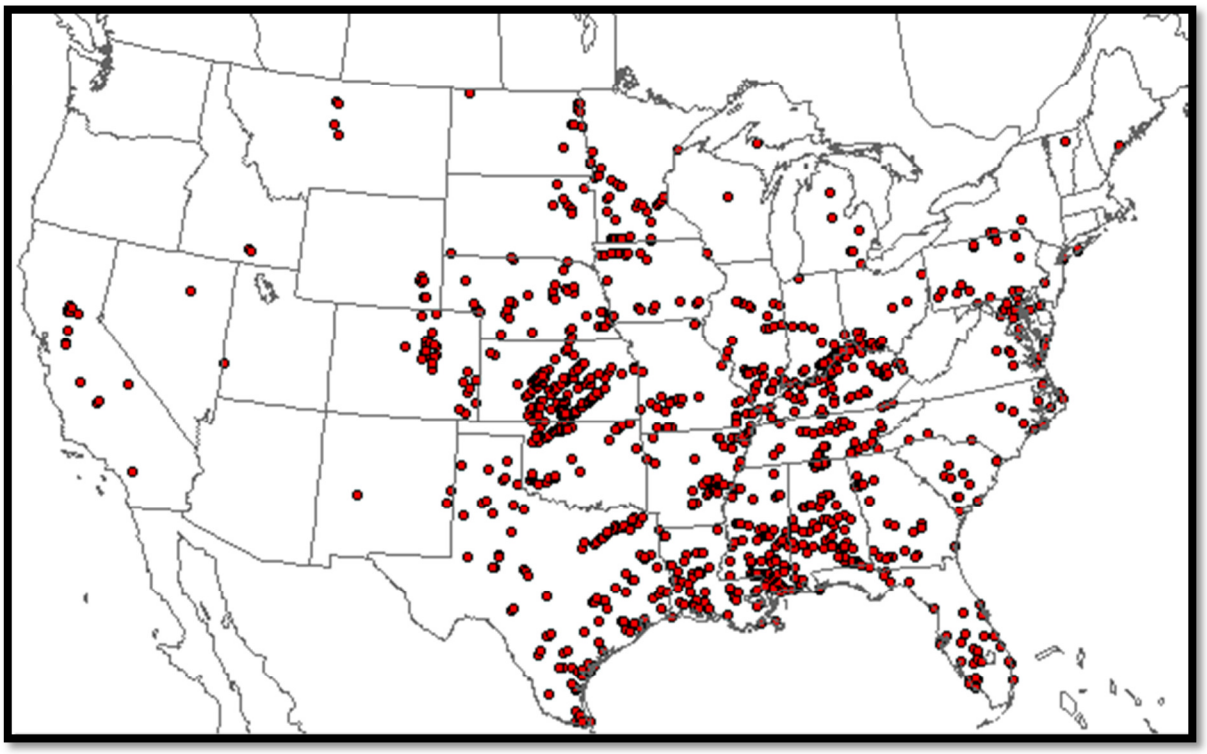

Figure 1.1 NOAA Storm Prediction Center's map of reported tornados 2012 (NOAA 2013)

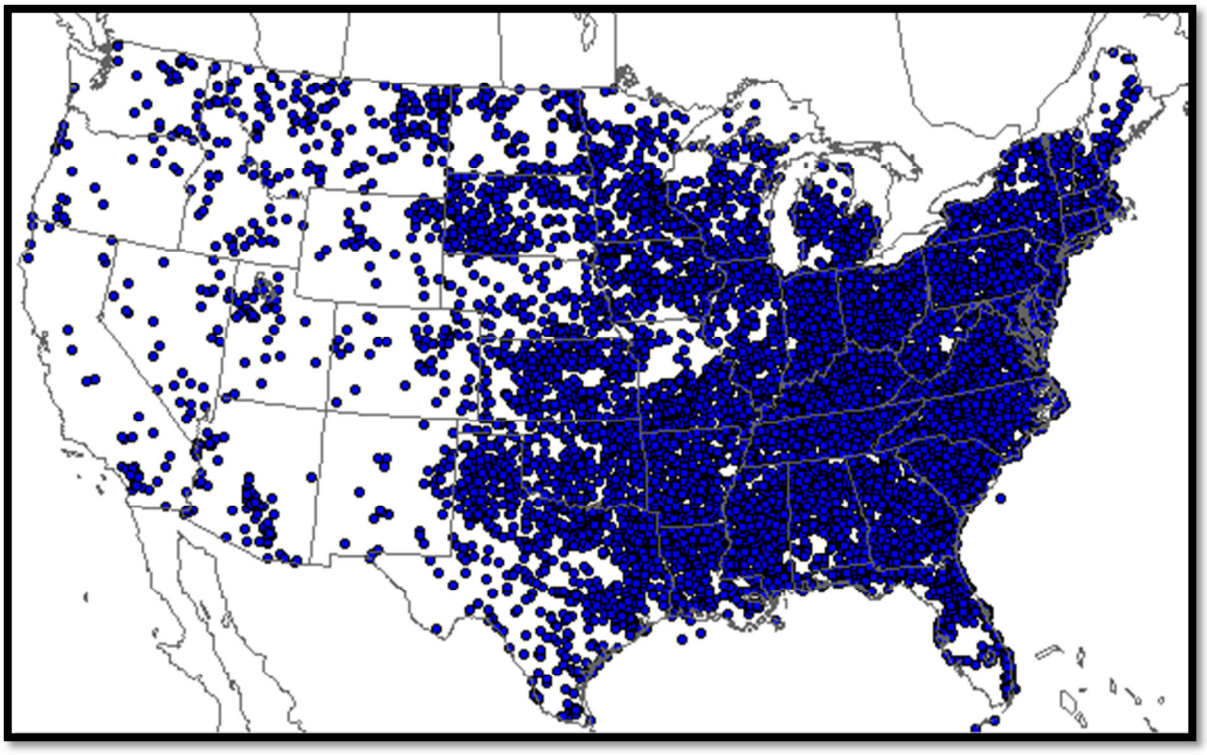

Figure 1.2 NOAA Storm Prediction Center's Map of extreme wind events shows extreme wind events are widespread across the U.S. (NOAA 2013)

2011 was a particularly active and lethal year for tornados with a total of 1691 tornados and 553 tornado fatalities (NOAA 2013). Accounting for many of these deaths was the Joplin, Missouri, tornado of May 22nd. This EF5 tornado forged a 7-mile damage path that razed 5000 buildings and killed almost 160 people, injuring another 1000 (Prevatt, et al. 2013).

The impacts also extend to significant economic losses as extreme wind events and tornadoes are responsible for a significant amount of damage, as illustrated in Figure 2.3 below. Of the $72.8billion of damages caused by natural catastrophes in 2011, tornadoes and thunder storms were responsible for $46.5 billion, or 64%. This compares to a paltry $257 million in overall losses caused by earthquakes, representing only about 0.4% of damage from all natural disasters. (Munich RE 2012). The economic impact of the Joplin tornado alone equaled $2.8 billion resulting in a nearly overwhelming burden for insurance companies, federal disaster response agencies, and the citizens charged with the rebuilding of their community (Associated Press 2012).

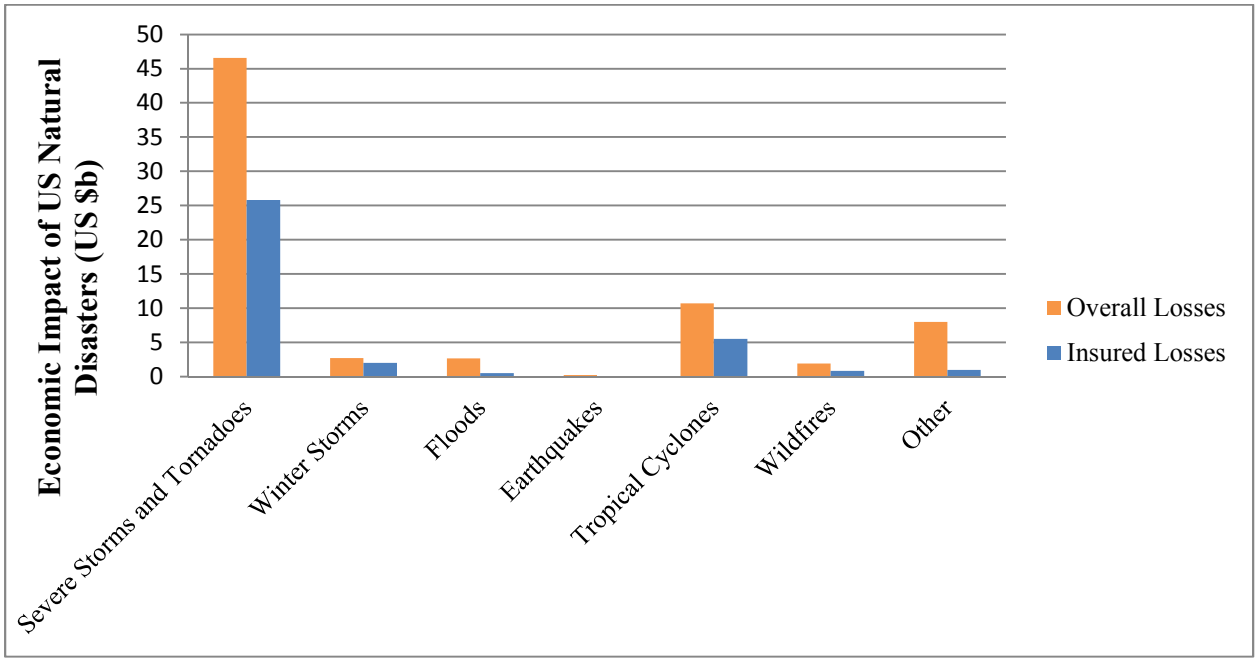

Figure 1.3The economic impact of tornadoes in 2011 was greater than the cost of all other natural disasters combined

The Great Plains Tornado Outbreak of May 3, 1999 produced 67 tornadoes responsible for 49 deaths and resulted in the development of a design guide for the construction of aboveground community and residential shelters; FEMA-361, *Design and Construction Guidance for Community Safe Rooms.* Released in July of 2000, FEMA-361 expanded on the design guidance provided in FEMA-320, *Taking Shelter from the Storm: Building a Safe Room inside Your House*, published 2 years earlier. FEMA-361 expanded on FEMA-320 to provide guidance for the design and construction of "community safe-rooms" in schools, hospitals, and other facilities capable of accommodating hundreds of occupants to provide "near-absolute protection" during an extreme wind event, namely, a hurricane or tornado. Now in its second edition, FEMA-361 sets forth two protection objectives: "protection against both wind forces and the impact of windborne debris" (FEMA P-361 2008).

The complex nature of tornadic winds dictates these two distinct design requirements. These winds are divided into three regions. The first region is near-surface, close to the vortex. Driven by the rotation of the tornado, winds in this region are extremely complex. Though still not completely understood, powerful rotating winds in the near-surface, close to vortex region create strong upward forces responsible for picking up and carrying debris, such as the 2"x4" timber used by FEMA to represent all tornado generated missiles. The second tornadic wind region is the near-surface, away from the vortex region, which combines the tornados rotational, inflow, and background winds. As distance from the tornado vortex increases, so too does dominance of the inflow winds over rotational winds, creating narrow bands of straight-line winds up to 250mph. Winds in this region, especially in these violent bands farther from the vortex, are responsible for the large forces which devastate most buildings. The third region is

above-surface. Though violent, these approximately circular winds are above the tops of most buildings (FEMA P-361 2008).

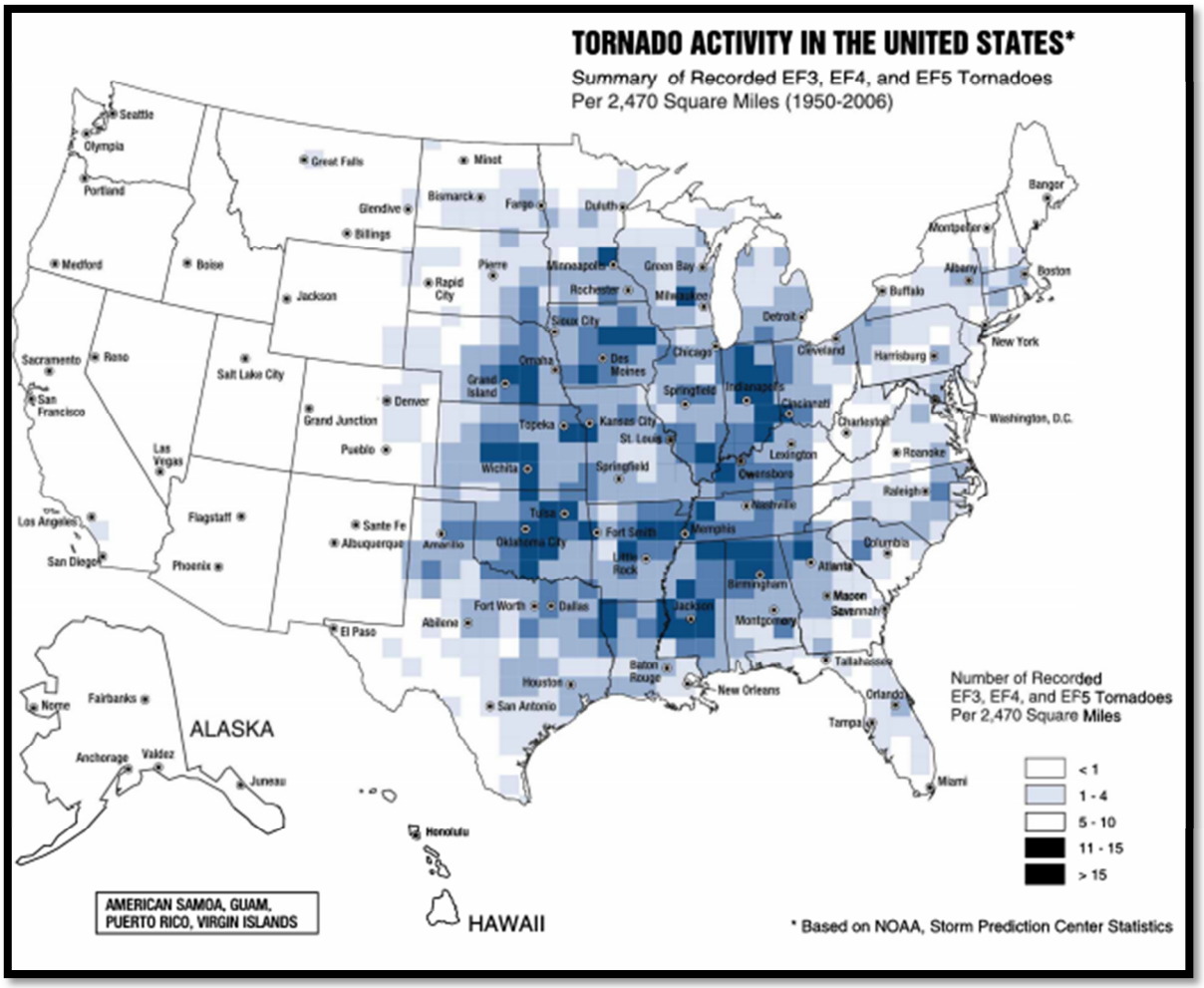

Figure 1.4 U.S. tornado occurrence density (FEMA P-361 2008)

Despite the seemingly random nature of a tornado's winds and its un-biased path of destruction, almost all structural failure can be accounted for by the collapse of low-rise buildings with light roofs and unreinforced masonry (URM) walls. This problem is further exacerbated when communities designate URM gymnasiums, churches, and lunchrooms as storm assembly areas, ignorant to the life-threatening inadequacy of URM to resist wind loads (Sparks, Liu and Saffir 1989). A perfect example can be seen in Figure 1.5, which shows the

post-tornado collapse of a school gymnasium whose structural system consists of URM walls and extremely light steel roof trusses. These circumstances present an urgent need to retrofit unreinforced and under reinforced masonry walls so that they can provide the "near-absolute protection" offered in FEMA-361.

One solution is to simply adapt the design guidance offered in FEMA-361 to retrofit the URM wall assembly. Coulbourne et al., (2002) provides retrofit design guidance as far as assessing the current structure to determine which parts of the building envelope require structural enhancement. When a wall diaphragm is identified as needing structural improvements, the authors offer two alternatives for adding flexural strength and debris impact resistance. The first strengthening method involves saw cutting the existing masonry wall and adding new reinforcing steel inside the concrete cells. This traditional method requires a large amount of time and skilled labor and disrupts the normal use of the facility. Adding reinforcing steel and concrete is also very costly. In fact, to strengthen all URM structures in the United States that need retrofitting would cost billions of dollars (Schmidt and Cheng 2009).

Unfortunately, if not mandated by the U.S. government or applicable building code, the significant investment required by the owner may prove too overwhelming and result in the choice to risk occupant safety and structural collapse rather than provide the needed retrofit. The second option for strengthening given by Coulbourne et al., is the application of fiber-reinforced polymer (FRP) strips or sheets on either side of the masonry. The high strength, low weight, durability, and availability of FRP laminates may lower the opportunity cost of reinforcing URM wall units and provide a comparatively inexpensive and easy way to retrofit masonry wall assemblies to successfully resist tornado wind pressures and debris impact, and provide

equivalent “near–absolute protection” provided by conventional strengthening techniques as described in FEMA-361 (Triantafillou 1998).

If an owner or engineer chooses this alternative reinforcement method, however, she will find little guidance on how to go about fulfilling these requirements. Though a large body of research in the field has led to design guidelines on using FRP to add flexural strength to masonry walls, how one would use these guidelines to meet FEMA’s stringent design requirements is vague. Even more unclear is how to go about using FRP to provide debris impact resistance to masonry walls. Though investigations into FRP behavior reveal its promise as a structural reinforcement material, any interpretation of how to apply these results is severely lacking. This leads to a desperate need for real-world, design applications on how to use FRP as reinforcement in the context of extreme wind events. Filling this void could provide the resource needed to diminish the economic impact of tornados and greatly improve the safety of this country’s masonry structures, and that is the goal of this thesis.

In the following chapters, the case will be presented for the application of FRPs to masonry structures in order to create safe rooms meeting the requirements of FEMA-361. In Chapter 2 a literature review will discuss current design guidelines and their limitations when considering tornadic loading, observed performance of masonry during a tornado, and current research on externally bonded FRP systems applied to masonry wall assemblies. This will make a case for using FRP as reinforcement for Tornado Safe Rooms, and clearly indicate insufficiencies of current design guidelines that might allow engineers to do so. Following an explicit statement of design assumptions and their consequences, Chapter 3 will compile the discussed research findings to create a set of design guidelines with the goal of increasing both out-of-plane bending strength and debris impact resistance. In Chapter 4, the applicability and

limitations of these newly developed and interpreted equations will clarify the intended scope for use of the new design guide. Additionally, a case study is performed to illustrate the valuable contribution this new set of guidelines makes to masonry design. This chapter ends with suggestions for further research, including an outline of protocol to follow to maximize effectiveness of further experiments.

Figure 1.5 Collapsed school gymnasium composed of URM and steel roof trusses (Mehta 1984).

Chapter 2 Literature Review

2.1 Current Design Guidelines Relevant to Masonry Buildings in Tornado Zones

FEMA-361 sets forth two protection objectives: "protection against both wind forces and the impact of windborne debris." To determine the loads acting on the structure and achieve its first protection objective, FEMA-361 dictates the use of the method outlined in ASCE 7-05, *Minimum Design Loads for Buildings and Other Structures*, providing a modified design wind-speed map, shown in Figure 2.2, adjusted load combination coefficients, and selecting specific design parameters. To protect against windborne debris, FEMA-361 requires that all roof and wall assembles be able to withstand the impact of a representative missile based on a testing procedure detailed in ICC-500, *Standard for the Design and Construction of Storm Shelters*. Through post-tornado investigations performed in conjunction with Texas Tech University, FEMA concludes this representative missile to be a 15lb, 2x4 timber with design impact speeds determined according to the safe room design wind speed map shown below (FEMA P-361 2008).

The second edition of FEMA-361 interprets the International Code Council's Standard for the Design and Construction of Storm Shelters (ICC-500), whose most recent edition was published in 2008. The document applies the guidance of ICC-500 to applicable U.S. codes, creating criteria for the design and construction of community and residential safe rooms, which it defines as "typically an interior room, a space within a building, or an entirely separate building, designed and constructed to provide life-safety protection for its occupants from tornadoes or hurricanes." Using more conservative design criteria, all FEMA safe rooms met or exceed the shelter requirements of ICC-500.These safe rooms can withstand both the high wind forces and debris impact associated with these extreme wind events. FEMA asserts that any safe

room designed to the specifications of this document provide occupants with “near-absolute protection,” that is, occupants have an extremely high probability of being protected from injury or death, and the publication claims no failures have been reported of a safe room constructed to FEMA criteria during an extreme wind event.

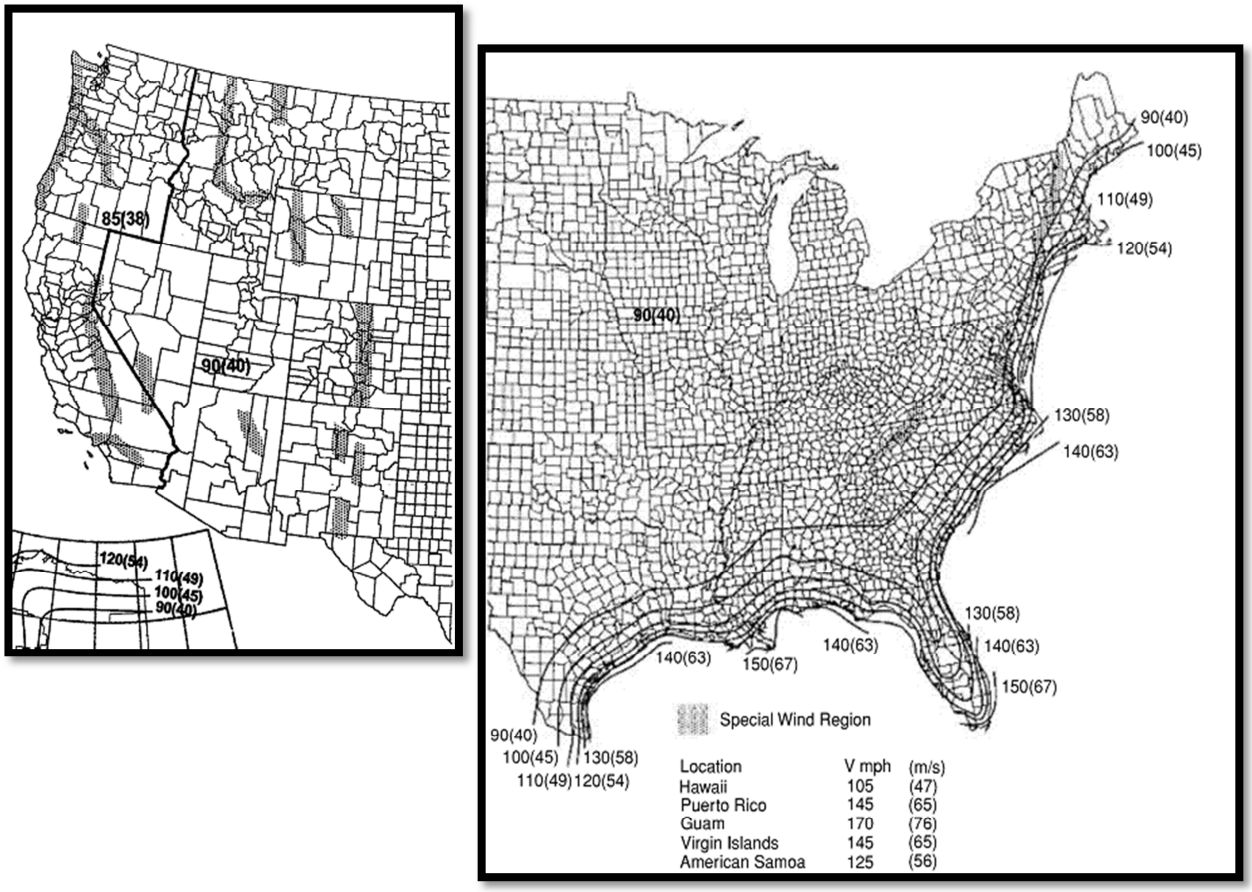

Figure 2.1 ASCE 7-05 Basic Design Wind Speed Map (ASCE 7-05 2005)

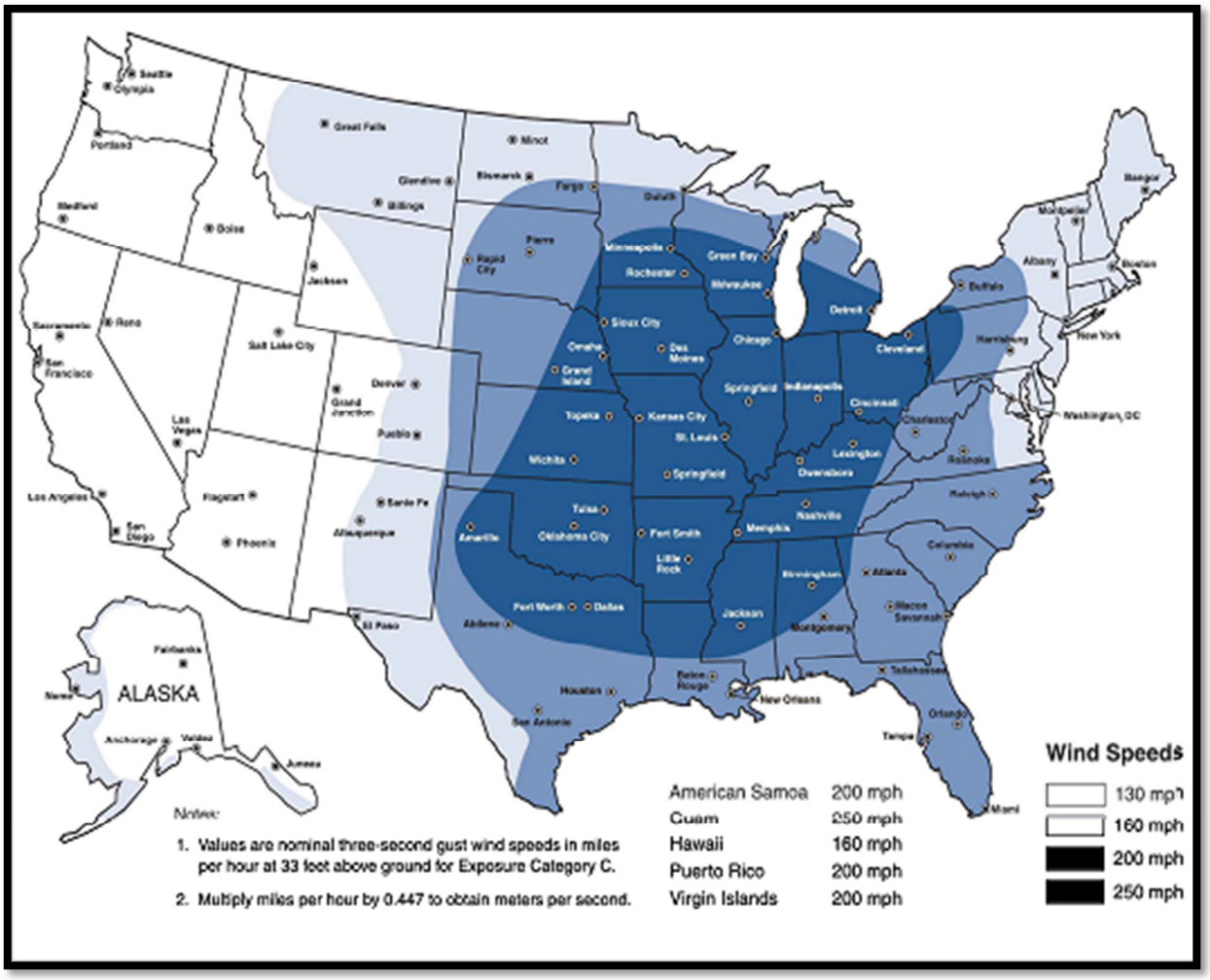

Figure 2.2 Fema-361 Tornado Safe Room Design Wind Speed Map (FEMA P-361 2008)

Table 2.1 Comparison of Basic Design and Tornado Wind Speeds

	ASCE 7	FEMA-361	Percent Change
Boston, MA	110 mph	160 mph	45%
Los Angeles, CA	85 mph	130 mph	53%
Montgomery, AL	100 mph	200 mph	100%
Joplin, MO	90 mph	250 mph	178%

In order to determine the forces acting on a structure during a tornado, FEMA-361 requires following Chapter 6, Method 2 of ASCE 7, "Analytical Procedure for Wind Loads." The design method is outlined in ASCE 7 section 6.5.3 and is explained below applying the parameters and alterations provided in FEMA-361.

1. **Determination of basic wind speed V and wind directionality factor K_d**

   Table 2.1 shows the design wind speeds of ASCE 7 compared to those of FEMA-361 for a tornado safe room for several different locations. This highlights the dramatic discrepancy in design requirements of the two documents. While the difference is less drastic in coastal areas that experience frequent, high straight-line wind gusts, in mid-western cities where the occurrence of tornados is much higher (see Figure 1.1) the difference is nearly 200%.

2. **Importance factor *I***

   The code explains that the *I* is used to adjust for different Mean Recurrence Intervals (MRI), associated with the probability that a structure will be affected by a certain event (exceedence probability). Because FEMA-361 uses an extremely high MRI of about 50,000 years with a .00002% exceedence probability, FEMA-361 assigns I=1.0.

3. **Exposure Category and Velocity Pressure Coefficient**

   The exposure category of a structure is based on the prevalence of surrounding vegetation, adjacent structures, or topographic effects. Due to the fact that most of these features will be razed in a tornado, FEMA designates use of Exposure Category C. Velocity Pressure Coefficients, K_z or K_h are determined using this exposure category and table 6.3 in ASCE 7.

4. **Topographic Factor K_{zt}**

   FEMA indicates $K_{zt} \leq 1.0$ as per ASCE 7 section 6.5.7.

5. **Gust Effect Factor G**

   As per ASCE 7 section 6.5.8, may be taken as G=0.85.

6. **Enclosure Classification**

   FEMA recommends classification of tornado safe rooms as partially enclosed.

7. **Internal Pressure Coefficient GC_{pi}**

   GC_{pi}=+/-0.85 is necessitated by FEMA as a conservative estimate for the change in atmospheric pressure felt by a structure in a tornado.

8. **External Pressure Coefficients C_p or Force Coefficients C_f**

   Determination of pressure coefficients follows ASCE 7 sections 6.5.11.2 and 6.5.11.3 and is dependent on area subject to wind load, relative location of loading, and classification of assembly as a Main Wind-Force Resisting System (MWFRS) or Components and Cladding (C&C). FEMA recommends use of MWFRS designation for wall assemblies subject to:

   - Axial, Shear, and Bending
   - Only Axial and Shear

   And for walls subject to only axial and bending loads

   - MWFRS for Axial
   - C&C for Bending

9. **Velocity Pressure q_z or q_h**

   Velocity pressure is determine using ASCE 7 eq. 6-15

$$q_z = 0.00256 K_z K_{zt} K_d V^2 I \left(\frac{lbf}{ft^2}\right)$$

This pressure is a function of the square of the wind speed *V,* hence, the difference flexural design capacity for a safe room designed to the standards of FEMA-361 and those designed for basic wind speeds is further exacerbated.

10. Design Wind Load F

As per ASCE 7 eq. 6-28

$$F = q_z G C_f A_f \ (lb)$$

Where q_z is the velocity pressure found in step 9, G is the gust factor of step 5, C_f is the force coefficient of step 8, and A_f is the total loaded area.

After determination of the design wind load, load combinations provide design load cases acting on the structure. Considering Strength Design (LRFD) the applicable load combinations from ASCE 7 section 2.3.2 are

3) 1.2D+1.6(L_r or S or R) +(L or 0.8W)

4) 1.2D+1.6W+L+0.5(L_r or S or R)

3) 0.9D+1.6W+1.6H

FEMA provides alternative coefficients to account for the distinction of designing for an extreme wind event with ultimate wind load W_x, rather than for a design level wind event with wind load W. FEMA replaces 0.8W with $0.5W_x$ in combination 3, and 1.6W with $1.0W_x$ in combinations 4 and 6 so that applicable load combinations for tornado safe room design become:

3)1.2D+1.6(L_r or S or R) +(L or $\mathbf{0.5W_x}$)

4) 1.2D+$\mathbf{1.0W_x}$+L+0.5(L_r or S or R)

6) 0.9D+$\mathbf{1.0W_x}$+1.6H

In order to satisfy the flexural loads on a wall assembly determined according to the above procedure (LRFD), one would look to ACI 530-08, "Building Code Requirements for Masonry Structures." Sections 3.2 and 3.3 of this governing masonry code provide flexural design requirements for unreinforced and reinforced masonry, respectively. Unreinforced masonry must satisfy:

$$F_{uc} \leq \phi F_{nc}$$

where

$$F_{nc} = 0.80 f'_m$$

Here, F_{uc} represents the ultimate compressive force, F_{nc} the nominal compressive force, f'_m is the compressive strength of the masonry unit, and ϕ is 0.6 as per section 3.1.4.2. Additionally, the tensile stress shall not be greater than the modulus of rupture, f_r, a property based entirely on the mortar used to bond masonry courses. For reinforced masonry, all tension is assumed to be carried by the reinforcing steel.

The second set of criteria which must be satisfied when designing a FEMA safe room is that for resistance to debris impact. As mentioned in Chapter 1, the cyclic winds of a tornado can generate missiles capable of penetrating structural systems leading to death or injury of its occupants or progressive collapse of the entire structural system as the interior surfaces are exposed to new wind pressures. In collaboration with the Wind Science and Engineering Research Center at Texas Tech University, FEMA designates a 15lb 2x4 wood timber as the representative missile for debris impact testing. Such a timber, approximately 12 to 14ft in length, was chosen after numerous post-disaster investigations due to its high potential to perforate conventional construction, and best represents other wind-borne debris such as roof tiles, metal roof panels, flashing, and billboard panels. Roof and wall assemblies must be

designed to resist the impact of this 15lb 2x4 wood member at the speeds given in Table 2.2 below. To prove that all roof and wall assemblies can successfully resist the debris impact at these design speeds, FEMA requires products used in these assemblies be tested in accordance with Chapter 8 of the International Code Council's Standard for the Design and Construction of Storm Shelters (ICC-500).

Table 2.2 Tornado Generated Missile Impact Criteria

Residential Safe Room	**Community Safe Room**	**Missile Impact Speed**	
Design Wind Speed		Vertical Surface	Horizontal Surface
250 mph	250 mph	100 mph	67 mph
--	200 mph	90 mph	60 mph
--	160 mph	84 mph	56 mph
--	130 mph	80 mph	53 mph

FEMA-361 made an important contribution to designing structures to withstand tornado loading. Of particular importance are its use of tornado occurrence statistics to provide modifications to the wind loading coefficients of ASCE 7-05, providing designers with a consistent and accurate method to determine structural load. FEMA-361 also gives an excellent set of prescriptive guidelines for using conventional construction methods to fulfill its requirements, and even explicitly lists reinforced masonry cross-sections which provide the required impact resistance. While a prescriptive method of design guidelines is clear and concise, it causes problems if one wishes to extend his design beyond the narrow scope of FEMA-361. The document provides guidelines modifying and retrofitting current spaces to become Safe Rooms, but identifies that many times it is not reasonable to strengthen walls against wind pressure and debris impact because of the high cost or restricted access. Although identifying this as a major retrofitting issue, that is where the guidance ends pointing to a major shortcoming

of the document. As discussed previously, it is the high cost and intensive labor of conventional retrofitting techniques using steel reinforcement that prevents most owners from taking action and strengthening masonry structures, resulting in so many catastrophic losses. Hence to need to fill this design gap by not only proving that FRP is an attractive alternative to steel for the retrofitting of masonry walls subject to tornado loading, but by indicating how this can be done as well.

2.2 Studies on the Performance of URM in Extreme Wind Events

Unreinforced masonry construction presents a major threat to life safety in the United States. A summary of evidence from 56 different wind and tornado damage reports conducted by researchers at Texas Tech found that structures composed of concrete masonry experienced a disproportionately large amount of catastrophic damage, even at wind speeds which only marginally exceeded design wind speeds (Mehta 1984). Several characteristics of typical URM construction account for this vulnerability.

First, unreinforced masonry structures are extremely rigid. This lack of ductility combined with zero redundancy for a one-story structure makes these assemblies extremely vulnerable to a tornados lateral and uplift forces. Second, though masonry structures have empirically shown to be quite resilient, some lasting for hundreds or even thousands of years, modern roof systems have become increasingly light. Previously, heavy roof systems, which transfer their load through the walls and into the foundations, pre-stressed concrete masonry wall assemblies. Thus, the negative uplift forces on the roof during a tornadic event only put the walls into decreased compression. However, as the weight of the roof system decreases, the pre-stressing in the masonry wall decreases, leading to an increase in the likelihood of the wall experiencing tension, and inevitable collapse when faced with the out-of-plane flexural loads

produced by an extreme wind event. This poor performance of concrete masonry units in tension is further exacerbated by the unreliability of the mortar used to bind the courses (Sparks, Liu and Saffir 1989). Finally, due to the Atmospheric Pressure Change (APC) experienced by a building in a tornado, the failure of one component, such as a wall or roof assembly, can lead to a progressive failure of the entire structure. This means that cracks or holes caused in masonry walls by windborne debris, even if these walls are not part of the MWFRS, leave the interior of the structure vulnerable to wind forces and can lead to a progressive failure of the entire structure (FEMA P-361 2008).

Figure 2.3 Tensile failure of masonry walled church (Sparks, Liu and Saffir 1989)

The real issue arises when communities designate unreinforced masonry structures, such as school or church cafeterias or gymnasiums, as tornado shelters despite their palpable inadequacy to resist tornado wind loading and debris impact (Sparks, Liu and Saffir 1989). Considering all of these issues, URM walls are subject to the most structural damage and pose the greatest threat to human life than all other structural systems subject to similar loading.

Unfortunately, the design wind speeds in ASCE-7 are much too low to provide any sort of protection during an extreme wind event. Unless a masonry structure is explicitly designed as a Safe Room in accordance with FEMA-361, it will be seriously vulnerable in the wind conditions created by a tornadic storm (Schmidt and Cheng 2009).

While resisting lateral wind forces is a major concern for community shelters with large, wind exposed surfaces, for small, residential safe rooms, providing enough impact resistance is likely the controlling design consideration. With conventional CMU reinforcement techniques, FEMA utilizes the results of impact resistance testing performed at Texas Tech. Using these findings, FEMA provides two sections which provide adequate impact resistance: 6in CMU reinforced with concrete and #4 rebar every cell and 8in CMU reinforced with concrete and #5 rebar 40in on center (every fifth cell). Additional TTU investigations found that unreinforced 8in and 12in walls fully grouted are able to stop penetration of the missile, but also experience cracking (McDonald 1990).

The strength of this body of research is that with so many extreme wind events per year, we have comprehensive understanding of how unreinforced masonry reacts to wind loads. The evidence clearly indicates that masonry designed using the empirical height to thickness design ratios is dangerous, and that loading marginally greater than the design load can be enough to cause a structural failure. It is know that the mechanism of failure is often mortar separation as the tensile capacities of mortar are unreliable, leaving the wall unable to carry tensile forces developed from suction on the roof, leeward, and side walls.

Furthermore, the design of masonry has developed so that it is possible to construct a masonry structure that performs brilliantly under tornado loading. FEMA's field investigations and impact tests provide the information needed for engineers to determine loads acting on the

structure, and ACI 530-08, Minimum Design Guide for Masonry Structures, can be used to ensure the masonry walls of the structure resist these loads. The weakness of these observations is that little is being done to bridge the gap between older, inadequately designed masonry structures, and structures designed to FEMA requirements.

While empirical evidence and controlled laboratory testing show the vulnerability of masonry to damage during tornados and other extreme wind events, it also, ironically, represents one of the only construction materials suitable for use in the construction of walls as part of a storm shelter. Due to the large negative pressures exerted on the roof of a structure during a tornado, steel must be used to connect wall and roof assemblies; leaving masonry and concrete as the only viable option for use in the construction of storm shelter walls (Coulbourne, Tezak and McAllister 2002). This paradox points to the obvious need to provide a solution to reinforce masonry so that it can properly withstand the flexural and debris impact forces of a tornado. Conventional reinforcing techniques, such as embedding rebar or attaching steel girders are time intensive and costly; however, the use of Fiber Reinforced Polymers applied as straps or sheets to the exterior surfaces of masonry walls represents an alternative with many advantages.

2.3 Use of FRP to Increase Flexural Strength of URM

The last fifteen years have seen numerous studies on the application of FRP laminates to retrofit URM walls in order to increase their resistance to out-of-plane bending. In these studies, unidirectional or woven fibers made of glass, carbon, or aramid (a heat resistant, synthetic fiber used in body armor) with extremely high tensile strength provide the necessary strength and stiffness. The matrix made of epoxy, polyester, or some other polymer compound, bonds and protects the fibers from damage and provides a mechanism for distributing load among the laminate. In a typical structural FRP Laminate, the matrix accounts for 40% of the total volume

(Velazquez-Dimas and Ehsani 2000). The combination of these two materials results in a lightweight material with high strength and stiffness in the direction of the fibers, high resistance to corrosion and fatigue, thermal resistance, relatively low cost, and which can easily be transported, handled, and installed (Triantafillou 1998).

These characteristics make FRPs an ideal choice to add flexural strength to unreinforced masonry walls subject to tornadic loading. In order to provide the best means to resist the high lateral loads experienced in such extreme wind events, research focusing on the amount of reinforcement, type of fiber, layout of fiber, surface preparation of the masonry surface, and anchorage of the FRP to the masonry will be discussed.

Amount of FRP Reinforcement

Triantafillou (1998) first determined the moment capacity of FRP reinforcement on masonry walls considering three common loading conditions, out-of-plane bending, in-plane bending, and in-plane shear all with axial force. For the case of out-of-plane bending, he introduced ρ_v, the ratio of FRP to total wall area and uses force equilibrium and strain compatibility to determine ω_{lim}, the limiting FRP fraction area.

$$\omega = \frac{(\varepsilon_{M,u} E_{frp})}{f_k} \rho_v \quad (1)$$

Where $\varepsilon_{M,u}$ is the ultimate compressive strain of the masonry, E_{frp} is the Young's Modulus of the FRP, and f_k is the masonry compressive strength. This limiting area represents the tipping point at which masonry crushing occurs simultaneously with FRP rupture. Solving for bending capacity of the new cross-section, it is shown that bending capacity increases with ω for low to moderate axial load levels, but decreases as ω increases for higher axial loads. It is concluded that for typical axial load values, masonry crushing is the likely mode of failure.

Albert et. al (2001) tested ten unreinforced, simply supported masonry walls with varying amounts of reinforcement of different types. Their results indicated that the deflection response of the composite Masonry-FRP system is divided into a non-linear phase followed by a linear phase until failure. The non-linear phase is controlled by the tensile strength of the mortar used, and its shape is dictated by the progressive transfer of load from a one joint to the next. After all joints have separated the behavior of the wall enters its linear phase, representing the contribution of the FRP until failure. This linear load-deflection behavior corresponds to a linear stress-strain relationship until failure, which is sudden and without any preceding plastic deformation. These responses are illustrated in Figure 2.4 and Figure 2.5 respectively. In order to determine the effect of the amount of fiber reinforcement, the reinforcement ratios were multiplied by the modulus of elasticity of the type of fiber used. This adjusted stiffness allowed for a comparison of specimens, leading to the conclusion that there is a one-to-one ratio between amount of FRP and stiffness.

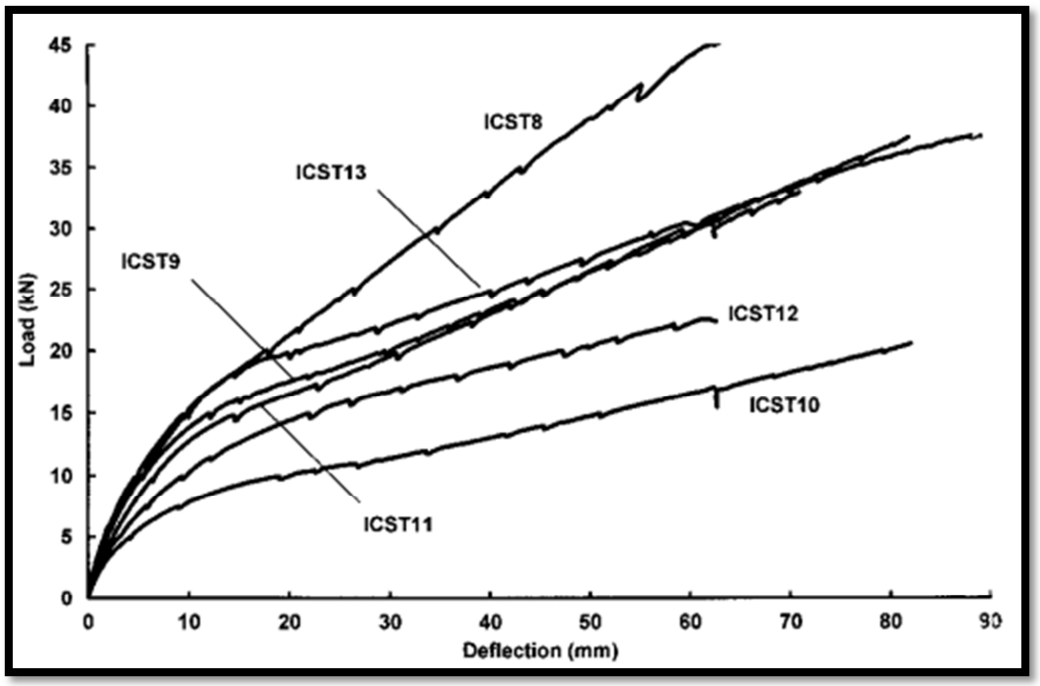

Figure 2.4 Load-Deflection diagram of FRP strengthened masonry (Albert, Elwi and Cheng 2001)

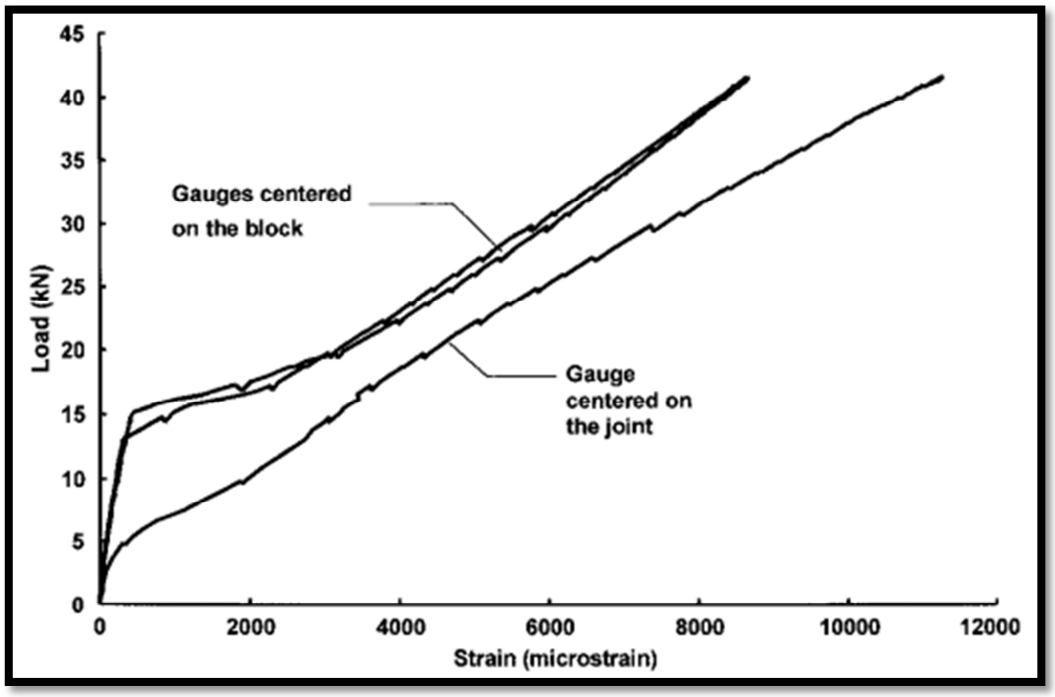

Figure 2.5 Stress-Strain curve of FRP strengthened masonry (Albert, Elwi and Cheng 2001)

Velazquez-Dimas and Ehsani (2001) also corroborate this linear elastic behavior in their application of cyclic out-of-plane loads to seven half-scale solid-brick masonry walls. Test specimens were divided into short walls with a height to thickness ration of h/t=14 and slender walls with h/t=28 in procedures controlling both load application and displacement. Experimenters determined a balanced reinforcement ratio using hook's law and equivalent stress, strain blocks, assuming the masonry fails in compression at a strain of 0.003 and the composite fails in tension at a strain of 0.02, with the balanced reinforcement condition ρ_b representing a simultaneous failure of the masonry by crushing and the FRP in tension. Experimental results found a linear increase in load with respect to the amount of reinforcement and FRP reinforced walls resisted up to 30 times their weight. Based on mid-span deflections and ultimate loads, they concluded the maximum reinforcement ratio for short walls be limited to 0.4 ρ_b and for slender walls 2 ρ_b.

Hamilton and Dolan (2001) applied out of plane loads to four "short" 6' high test walls and two "tall" 15'4" test walls all simply supported and composed of 8" CMU strengthened with Glass Fiber Reinforced Polymer (GFRP) reinforcement. After deriving a balanced coverage ratio of:

$$\alpha_c = \frac{b_g}{b} = (0.85)^2 t \left(\frac{f'_m}{f_{gu}}\right)\left(\frac{\varepsilon_{mu}}{\varepsilon_{mu}+\varepsilon_{gu}}\right) \quad (2)$$

where α_c is the coverage ratio, b_g is the total width of FRP and b the width of the wall, f_{gu} is the load capacity of the composite in units of force/unit width, $f_m^{'}$ is the compressive strength of the masonry and ε_{mu} and ε_{gu} the respective strain capacities for masonry in tension and FRP in tension. The value of α_c indicates how much of the wall will be covered in a single layer of enforcement, and for design ratios less than this the flexural capacity is predicted as

$$M_n = T_{gu}\left(d - \frac{a}{2}\right) \quad (3)$$

$$a = \frac{T_{gu}}{0.85 f'_m b}; T_{gu} = b_g f_{gu} \quad (4)$$

where T_{gu} is the tensile capacity of the strap and a is the depth of the equivalent stress block. For the over-reinforced condition where the design ratio is greater than that given by α_c

$$M_n = 0.85 a b f'_m \left(\frac{c}{2}\right) \quad (5)$$

where c is the thickness of the face shell. Researchers proposed that the under-reinforced failure mode of FRP fracture is the more desirable failure mode because it prevents designers from needing to acquire an estimate of the masonry strength and because each FRP strip provides redundancy. Their results found that by reinforcing un-grouted CMU walls with four strips of GFRP (an under-reinforced condition leading to GFRP fracture), the increase in bending stiffness was equivalent to a similar 8" CMU wall with #5 steel rebar spaced every 24in. These important results indicate that even for unreinforced walls with large aspect ratios, FRP

reinforcement can prove just as effective as conventional reinforcing steel. This notion is further corroborated by Hamoush et. Al (2001) who found a strength increase of over 1000% for walls reinforced with Glass Fiber Reinforced Polymer compared to the unreinforced condition.

Tan and Patoary (2001) tested 30 masonry walls in five series and increased the amount of fiber reinforcement on a wall by doubling the layers of reinforcement form two to four. Table 2.3 summarizes the results for the different reinforcement types and shows that the presence of FRP reinforcement significantly increases the wall's flexural strength, and that load carrying capacity increased by 45% for walls strengthened with GFRP and when two additional layers of laminate are applied to the wall assembly.

Table 2.3 Comparison of failure loads of CMU walls reinforced with multiple layers of FRP

	Layers of Reinforcement		
Reinforcement Type	0	2	4
Unreinforced	20.1 kN	--	--
GFRP	--	97.1 kN	140.9 kN
CFRP	--	43.0 kN	62.5 kN

Fiber Type

Triantafillou (1998) comments that the combination of high-stiffness and light weight makes carbon, glass, and aramid fiber reinforced polymers an outstanding construction material, especially in considering their application to the reinforcement of existing masonry structures. In the determination of normalized FRP fraction area ω shown in Eq. 1, it is shown that an increase in ω, and hence an increase in out-of-plane bending capacity for walls experiencing reasonable axial loads, depends on the product of the fiber stiffness E_{frp} and reinforcement ratio ρ_v. This leads to the conclusion that the stiffer the laminate, the more efficient its performance indicated by a lower reinforcement ratio.

Albert et. al (2001) also performed a series of experiments focusing on the performance characteristics of carbon versus glass fibers. Table 2.4 shows a comparison of the three different reinforcement types, glass sheet, carbon sheet, and carbon strap (a much denser distribution of carbon fibers resulting in much higher stiffness per unit width)

Table 2.4 Comparison of glass and carbon reinforcement under out-of-plane flexure

	Stiffness (kN/mm)	Maximum Load	Failure Mode
Glass Sheet	32.1	28.9	N/A
Carbon Sheet	238.1	36.0	Flexure-Shear
Carbon Strap	34.5	46.4	Flexure-Shear

Figure 2.6 compares the response of these different reinforcment types, and shows the same two phase response found in their experiments controlling for amount of fiber, illustrated in Figure 2.4. Additionally, the carbon sheet and strap all failed in a combined flexure-shear mode, as did the wall strengthened with glass sheet after being retested under cyclic load.

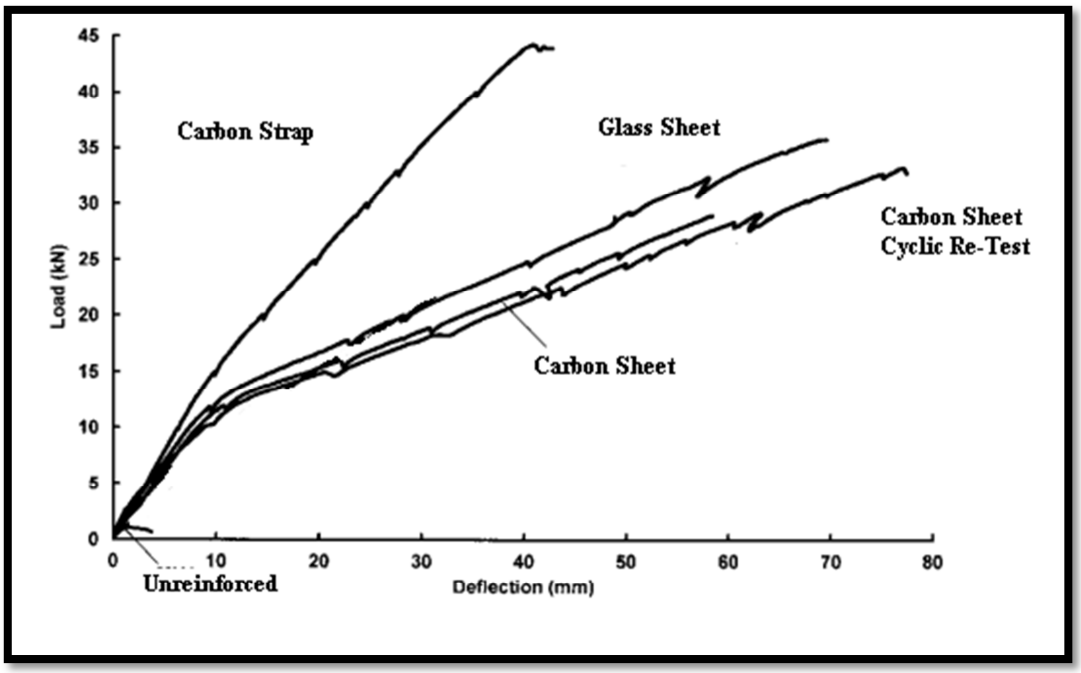

Figure 2.6 Load Deflection Response of different FRP fibers (Albert, Elwi and Cheng 2001)

Tan and Patoary (2004) also found similar responses among glass and carbon fiber reinforced polymers and both are capable of dramatically improving the performance of an unreinforced masonry wall, but indicate that surface preparation and FRP thickness have a much greater effect on the failure mode and ultimate load carrying capacity.

Fiber Layout

Albert et. al (2001) tested walls reinforced with carbon sheets applied in strips of various widths to a wall with a diagonal reinforcement ratio. Researchers concluded that the fiber layout had little effect on overall flexural behavior of the wall; however, due to the varying reinforcement ratios among the walls tested, these experiments are poorly controlled to determine the best type of reinforcement layout.

The experimental program of Hamoush et. al (2001) compared vertical strips of aramid-fabric in two layers forming an orthogonal grid with two layers of continuous woven glass fabric. The results point to the continuous woven web reinforcement providing a greater contribution to flexural strength, outperforming the walls with unidirectional strips in an orthogonal grid by about 8%.

Tan and Patoary (2004) also compared orthogonal and diagonal alignment of Carbon Fiber Reinforced Polymer CFRP strips and found that each failed at the same failure load. Though significantly increasing the flexural out of plane capacity over the unreinforced wall by more than 200%, the bond surface of the masonry was unprepared and both specimens experienced FRP debonding as the primary failure mode. It is important to note that this premature failure mode in which the FRP separates from the masonry surface is not desirable and means that the reinforcement fibers did not reach their maximum tensile strain values.

Bond Surface Preparation

The results of Tan and Patoary (2004) indicate that FRP applied to an unprepared masonry wall without providing anchorage will fail due to FRP debonding regardless of reinforcement layout. Velazquez-Dimas and Ehsani (2000) also found that delamination of the FRP reinforcement from the masonry surface to be the dominate mode of failure, even in specimens reinforced to two times the balanced condition. Although these experiments tested brick masonry wall assemblies, it indicates that no matter the quantity, type, and layout of FRP reinforcement used to strengthen a masonry wall is irrelevant if a proper bond cannot be created. This bond is a key parameter in accurately predicting the desired failure, either masonry crushing in the over-reinforced case or FRP rupture in the under-reinforced case. Additionally, in developing their models for flexural strength of FRP strengthened CMU, most experimenters assume a no-slip condition between the two systems, further indicating that the first critical decision in strengthening of Masonry with FRP is surface preparation and anchorage techniques to increase the bond strength at this interface.

In their testing of 15 walls of 8" CMU reinforced with GFRP strips and sheets, Hamoush et. al (2001) tested two surface preparation techniques: sand blasting and cleaning with a wire brush. The surfaces of six of the wall assemblies were sandblasted and another six were manually cleaned with a wire brush, after which all specimens were sprayed with a water jet to remove dust and allowed to dry for 48 hours before the application of the epoxy matrix.

Figure 2.7 compares the effect of these two preparation techniques on the maximum flexural load carried by the wall at failure. It is important to note that none of the 12 walls that underwent surface preparation experienced a failure by delamination, the failure mode indicative of poor bond strength. Researchers concluded that both surface preparation techniques allowed

for the development of sufficient bond strength between matrix resin and CMU, but note that neither technique significantly increases strength over the other. Unfortunately, the experiment does not control for surface preparation, and provides no test sets including unprepared surfaces with unidirectional and web fiber reinforcement.

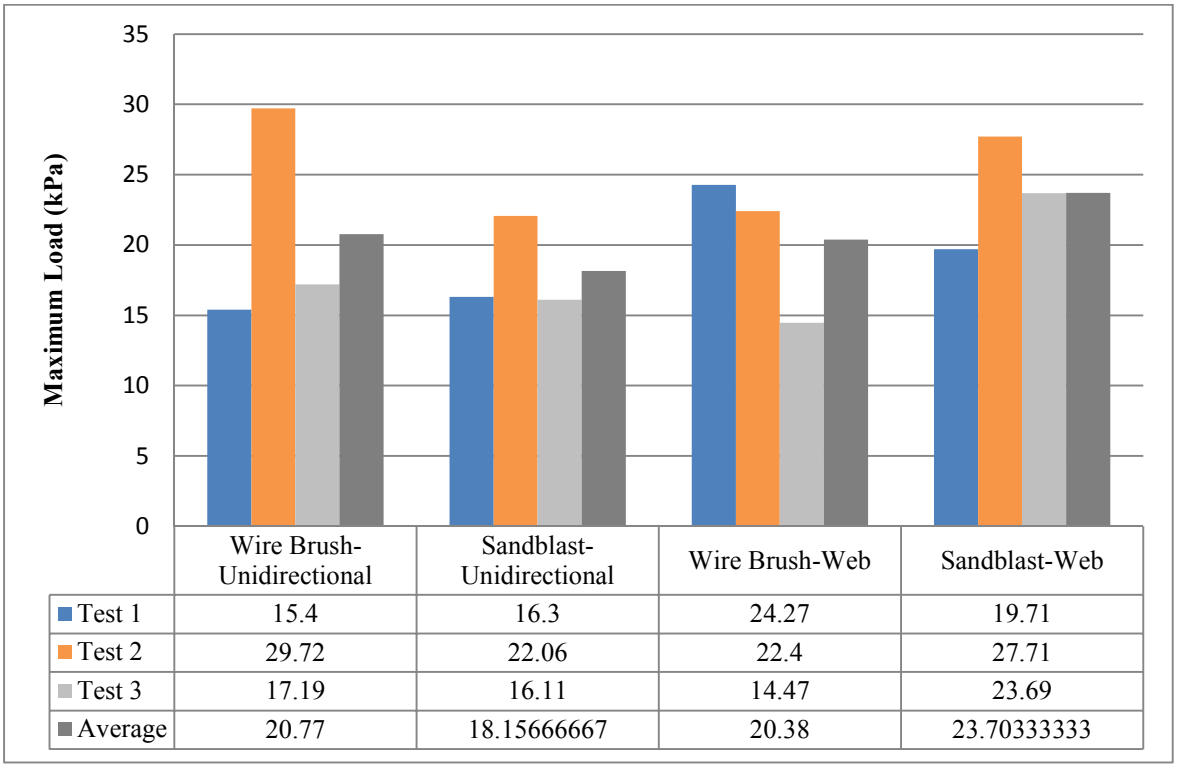

	Wire Brush-Unidirectional	Sandblast-Unidirectional	Wire Brush-Web	Sandblast-Web
Test 1	15.4	16.3	24.27	19.71
Test 2	29.72	22.06	22.4	27.71
Test 3	17.19	16.11	14.47	23.69
Average	20.77	18.15666667	20.38	23.70333333

Figure 2.7 Comparison of sandblasting and wire brushing masonry surface preparation on bond strength

Tan and Patoary (2004) accounted for surface preparation in their testing of 110mm thick brick masonry walls comparing the effect surface grinding of the masonry surface on the flexural capacity among their various reinforcement layouts and fiber types. By grinding the surface, experimenters hoped to rough the masonry and improve bond strength.

Table 2.5 and Figure 2.8 show relevant experimental results. Not surprisingly, all assemblies with unprepared surfaces failed prematurely due to FRP debonding. This indicates the necessity of surface preparation prior to application of the laminate reinforcement.

Table 2.5 Effect of surface grinding on flexural strength of FRP reinforced masonry

Series	Specimen	Reinf. Type	Surface Prep	Failure Load	Failure Typ.
III	GUG	Glass Fabric	None	61.0	Debonding
	GG	Glass Fabric	Ground	91.5	Punching Shear
	CUG	Carbon sheet	None	62.5	Debonding
	CG	Carbon Sheet	Ground	108.2	Punching Shear
IV	GUGU	Glass Fabric	None	46.5	Debonding
	GGU	Glass Fabric	Ground	199.5	Flexural Compression
	CUGU	Carbon Sheet	None	88.0	Debonding
	CGU	Carbon Sheet	Ground	184.3	Flexural Compression

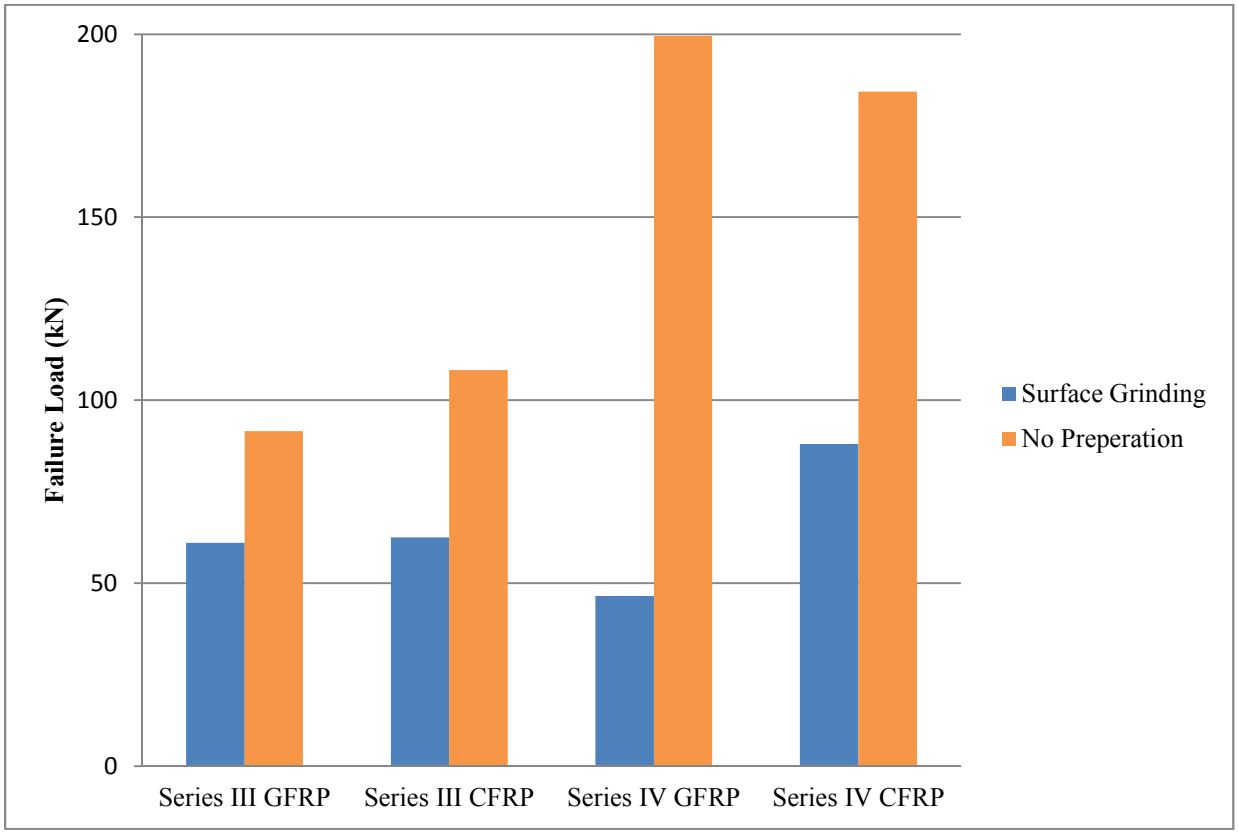

Figure 2.8 Comparison of surface grinding and unprepared surfaces on bond strength

The difference between Series III and Series IV results lies in the type of load application. Series III walls were subject to concentrated load while Series IV walls were subject to a uniform load applied with an airbag. For the purpose of considering the pressure exerted on a wall assembly in a tornado, the results from Series IV are more applicable, though results from both tests are included for clarity and completeness.

One must be cautious when extrapolating these results, which test brick masonry, to concrete masonry, due to the difference in the inherent porous nature of the two surfaces. However, by comparing these results with other experimental failure modes, such as those observed by Velazquez-Dimas and Ehsani (2000) who found delamination as a predominant failure mode for unprepared masonry walls, these new results on surface grinding become quite relevant.

Camli and Binici (2006) examined the effect that a plaster finish can have on a masonry wall strengthened with CFRP subject to shear imposed by the loading of two 280mm x 180mm steel plates. The test specimens had a single strip of CFRP reinforcement of varying width and length bonded horizontally to the wall's centerline. 39 of these shear double-push out tests were performed on solid concrete blocks of both low strength (10MPa) and normal strength (30MPa) concrete, and another 15 on hollow clay tile units. All surfaces, either plain concrete, tile, or plaster finish, were blown with air to clear any dust prior to application of the CFRP strips. Figure 2.9 below compares the effect of this added plaster layer controlling for other experimental parameters (unit width and bond length and width) and shows even a thin layer of plaster adversely affects the strength of the wall.

All specimens failed by debonding, and for the plain surface assemblies, this happened at a much lower loading than the solid concrete blocks, indicating that discontinuities in masonry texture and the presence of ungrouted cores can weaken the FRP/Masonry bond. Failure of plaster finished walls occurred at much lower loading, and occurred by debonding at either the CFRP/plaster or plaster/concrete interface. Researchers found the average bond strength for plaster finished assemblies to be about 10-20% of the total CFRP tensile strength, compared to 40%, 53%, and 31% for plain surfaced low strength concrete, regular strength concrete, and hollow tile masonry respectively.

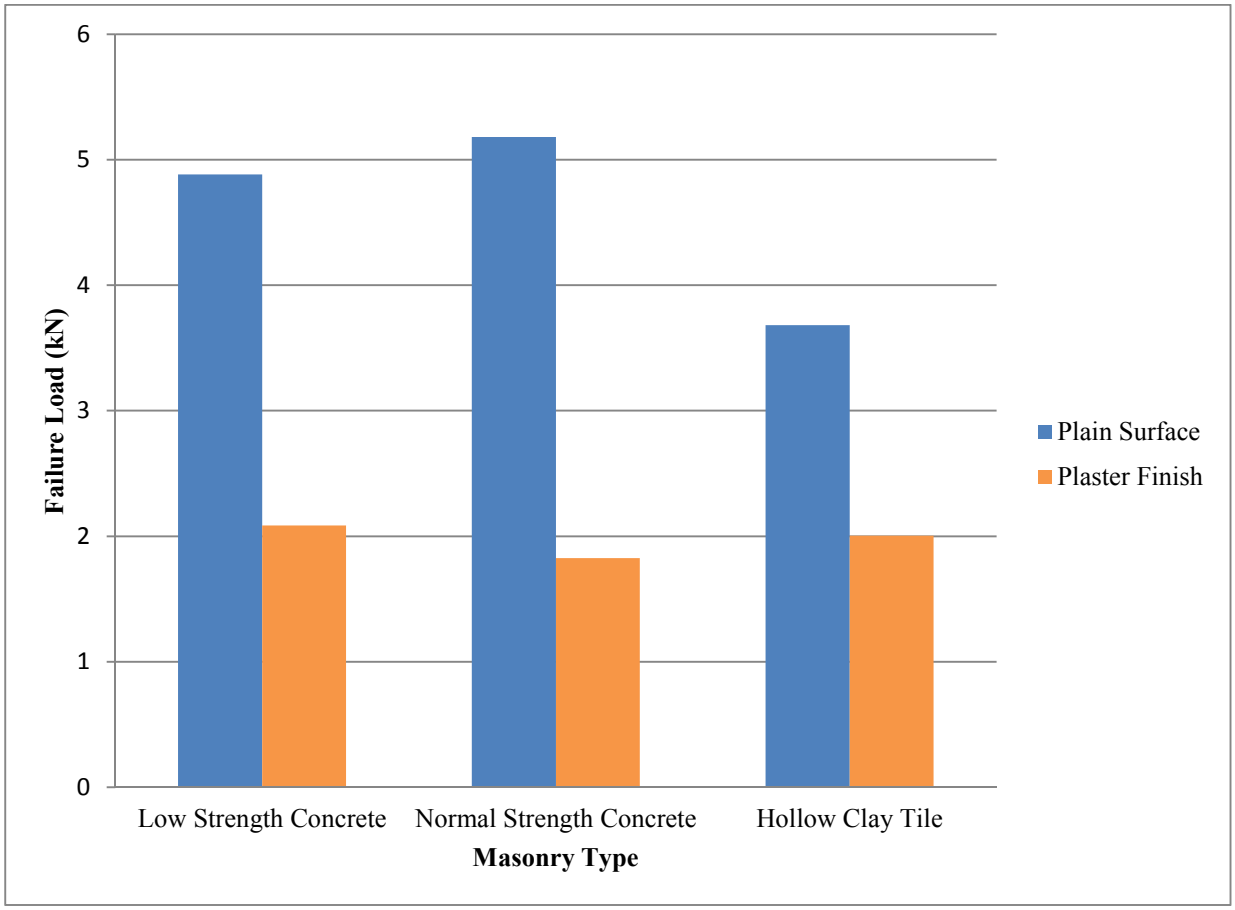

Figure 2.9 Effect of plaster finish on CFRP reinforced concrete and hollow clay tile masonry

Anchorage of FRP to Masonry

Epoxy is used to bond FRP strips to masonry in most cases; however, some have also investigated the use of additional anchorage. Tan and Patoary (2004) compared the results they obtained for flexural strength of FRP reinforced walls with and without surface preparation to walls utilizing both fiber anchor bolts and a steel bar anchorage system. The fiber anchor bolts were installed between the first and second layers of fiber reinforcement into pre-drilled inclined holes, and spaced evenly along the perimeter of the wall. Each wall had 28 glass fiber bolts measuring 100mm in length and 8mm in diameter. Similarly, the steel bar anchorage system used pre-drilled grooves along the wall's perimeter to install a steel rod between the first and second layers of FRP laminate.

Figure 2.10 compares the contribution of these anchorage systems to the load carrying capacities of the FRP strengthened masonry wall in flexure to the unprepared and surface ground walls discussed in the previous section. While the unprepared surfaces failed by debonding of the FRP from the masonry substrate, all six of the other specimens failed due to flexural compression of the concrete, one of the two desired failure modes. Because of the significant increase in flexural strength provided by adding surface preparation or an anchorage system to the application of the FRP, the authors concluded that either surface grinding or an anchorage system should be used to increase load carrying capacity and ensure the onset of the desired failure mode.

Camli and Binici (2006) employed embedded anchorage and fan anchorage to their test specimens of concrete prisms and hollow clay tiles reinforced with CFRP sheets. For the solid concrete units, the embedded anchor was achieved by bonding the CFRP sheets to the inside of pre-drilled holes which were then filled with epoxy. For the hollow clay tiles, the CFRP was

attached to anchor dowels, epoxied, and finally placed into pre-drilled holes. The fan anchorage involved spreading out the ends of the CFRP sheet into a fan shape to provide a larger bonding surface.

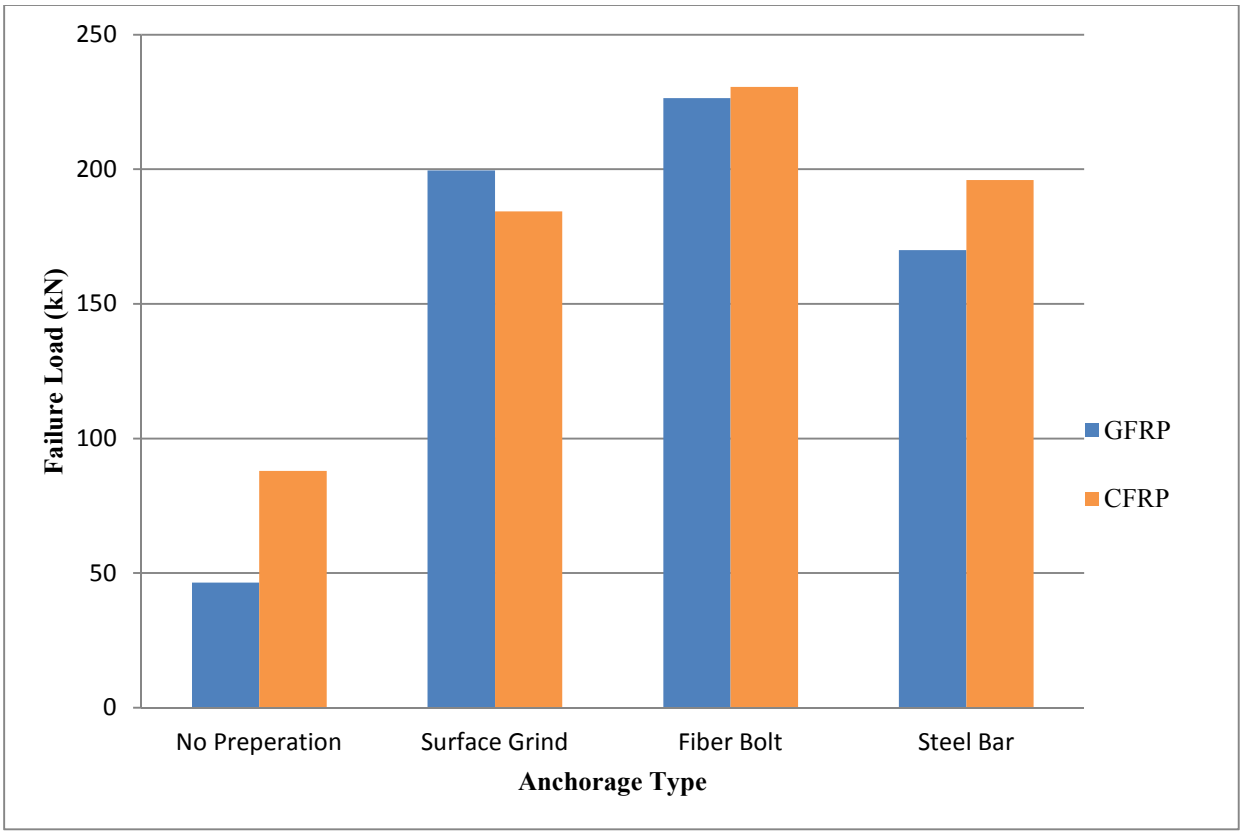

Figure 2.10 Load carrying capacities of different anchorage system and surface preparations under uniform load

Use of embedded anchors for all plaster finished and unfinished surfaces resulted in failure modes of either masonry compression or FRP rupture, indicating that embedment should be used if strengthening a finished masonry wall. Researchers also found that the embedded anchors provided up to double the flexural strength of the standard epoxy application,

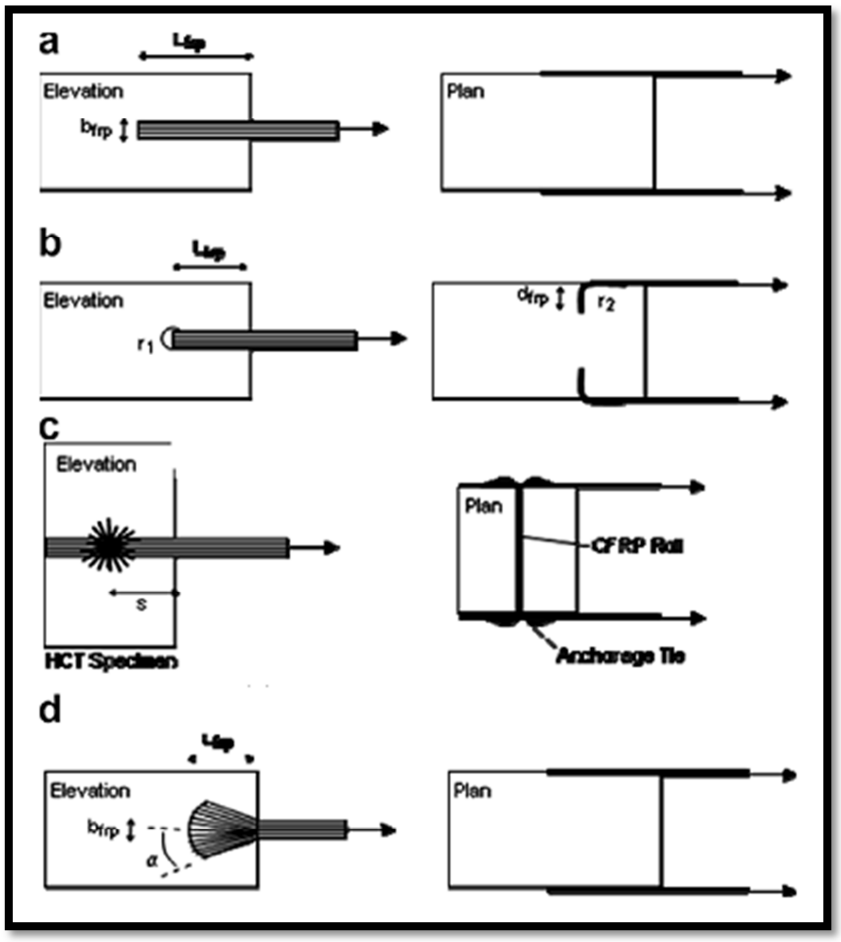

Figure 2.11 Anchorage Layouts (a) Standard epoxy bond, (b) Embedded anchor for concrete unit, (c) embedded anchor for hollow clay tile, (d) fan anchor (Camli and Cinici, 2006)

independent of compressive strength of the masonry or embedment depth beyond a certain effective length, around 25mm. Results of the fanning of the FRP strips at either end showed only a moderate improvement in increased wall flexural strength, and spreading the fibers at an angle greater than 30° actually decreased the strength of the composite system due to a concentration of stresses in the spread angle, leading to premature FRP rupture. This lead to the conclusion that this fan type anchorage of CFRP strips should be avoided, while embedment is preferred, especially in the case of a plaster finished masonry surface.

Flexural Design Guidelines

Two documents summarize this body of evidence into design guidelines for the strengthening of masonry to resist out-of-plane loads. Galati et. al, (2005) provides design equations for the flexural capacities of load-bearing and non-load bearing walls based on force equilibrium and strain compatibility.

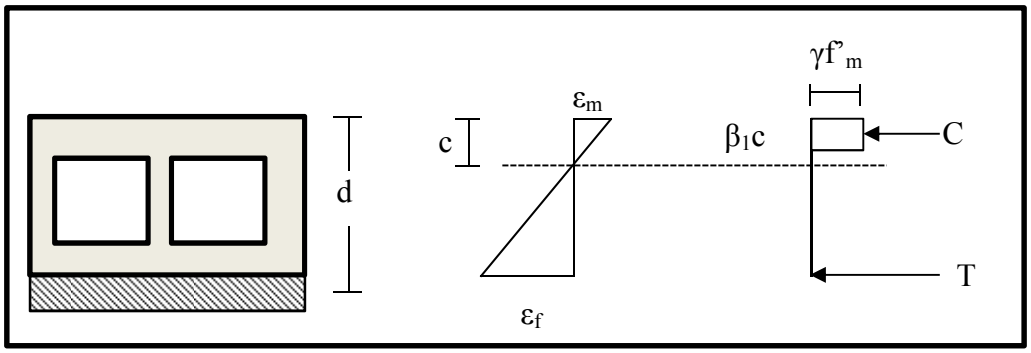

Figure 2.12 Strain and equivalent stress block for FRP reinforced masonry

For non-load bearing walls, the strain distribution illustrated above gives:

$$\frac{\epsilon_m}{c} = \frac{\epsilon_f}{d-c} = \frac{(\epsilon_m+\epsilon_f)}{d} \tag{6}$$

For which the corresponding stress distribution can be calculated using the Whitney Stress Block:

$$C = T \tag{7}$$

$$(\gamma f'_m)(\beta_1 c)b = A_f f_f \tag{8}$$

The scenario where crushing of the masonry and FRP rupture occur simultaneously is represented by:

$$\rho_{fb} = \gamma\beta_1\left(\frac{f'_m E_f \epsilon_{mu}}{f_{fe}E_f\epsilon_{mu}+f_{fe}}\right) \tag{9}$$

f_{fe} and ε_{fe} are the effective design strength and strain, and are found by multiplying the tensile strength and strain provided by the manufacturer by an environmental reduction factor C_E and a bond reduction factor k_m. The FRP reinforcement ratio for a strip of masonry wall is given by the ratio of total reinforcement area to wall cross-sectional area:

$$\rho_f = \frac{A_f}{bt} \tag{10}$$

When the amount of reinforcement results in a reinforcement ratio which is greater than the balance condition, $\rho_f > \rho_{fb}$, then masonry crushing is the controlling failure mode and the moment capacity for a section of masonry wall of width b can be found by summing internal forces:

$$M_n = (\gamma f'_m)(\beta_1 c) b \left(d - \frac{\beta_1 c}{2}\right) \tag{11}$$

For the case where $\rho_f < \rho_{fb}$, FRP rupture is the controlling failure mechanism and determination of flexural strength becomes an iterative process based on an initial determination of the location of the neutral axis, c. An iterative process is suggested to find c along with the compressive strain in the masonry at failure, ε_m, as well as the values for β_1 and γ. However, if one assumes the location of the neutral axis at the balanced reinforcement condition, Eq. (5) can be arranged giving:

$$c_b = \left(\frac{\varepsilon_{mu}}{\varepsilon_{mu} + \varepsilon_{fe}}\right) d \tag{12}$$

This value is then used to find flexural capacity based on FRP rupture:

$$M_n = A_f f_{fe} (d - \frac{\beta_1 c_b}{2}) \tag{13}$$

When a CMU wall is load bearing, the effects of axial stress must be considered. For this case, the balanced reinforcement ratio becomes:

$$\rho_{fb} = f'_m [\gamma \beta_1 \left(\frac{E_f \varepsilon_{mu}}{E_f \varepsilon_{mu} + f_{fe}}\right) - \frac{P_u}{b t f'_m}] \tag{14}$$

Adding the effects of axial stress results in new equations for nominal flexural capacity of masonry crushing failure can be expressed in terms of either masonry compression or FRP tension:

$$M_n = (\gamma f'_m)\beta_1 cb\left(d - \frac{\beta_1 c}{2}\right) - P_u(d - \frac{t}{2}) = A_f f_f \left(d - \frac{\beta_1 c}{2}\right) + P_u\left(\frac{t}{2} - \frac{\beta_1 c}{2}\right) \quad (15)$$

And, for the case of $\rho_f < \rho_{fb}$ where FRP rupture is the controlling failure mode, the authors suggest use of a similar iterative process to determine the equivalent stress block as described for non-load bearing walls, or using a simplified procedure and taking β_1 and γ equal to 0.80 as prescribed by ACI 530 and solving for the right hand side of Eq. 14 above.

The Guide for the Design and Construction of Externally Bonded Fiber-Reinforced Polymer Systems for Strengthening Unreinforced Masonry Structures, ACI 440.7R-10, adopts most of the design equations used by Galati et al. (2005) in addition to providing detailing requirements, where it suggests the use of an anchor embedment similar to that tested by Camli and Binici (2006), FRP reinforcement layouts for shear and bending reinforced walls, and several useful design examples.

The body of evidence of FRP reinforcement of masonry to resist out of plane loads presents a strong case for its use as a means of reinforcing URM walls to resist tornado loads. Due to its incredibly high tensile strength, enough FRP can easily be applied so that the mode of failure for a masonry wall in out-of-plane failure mode is crushing of the masonry. The area of reinforcement at which masonry crushing occurs simultaneously with FRP fracture is known as the balanced reinforcement ratio and affected by the relative stiffness of the type of fiber used, meaning that walls reinforced with CFRP will require less total area of reinforcement. When applying the design guidelines such as ACI 440.7R, or those of Galati, et. al (2005), designing for this over-reinforced condition is preferable in Safe Room design as life safety is the ultimate

concern, and warnings of structural failure are of little aid to the occupants during an extreme wind event. It is also determined that the reliability of a desired failure mode occurring can be enhanced through masonry surface preparation and various anchorage systems.

This research, however, only addresses one of the loading conditions experienced during a tornado and this represents the major weakness of the studies discussed above. The intention of most researchers was too broad and dealt only with retrofitting walls to increase flexural capacity, with FRP being a desirable choice because of its low cost and availability. If researchers did set out with intention, it was to determine FRPs applicability in the case of seismic loading in which FRP is advantageous for its low strength to weight ratio. In either case, though experimental procedures control for many different variables and provide strong evidence for using FRP to add flexural strength to masonry walls, this alone is not enough to conclude that FRP is a desirable or adequate solution for reinforcing the walls of Tornado Safe Rooms.

2.4 Use of FRP to Increase Impact Resistance of URM

While numerous studies investigate the contribution of fiber reinforced polymers to the flexural strength of an unreinforced masonry wall, a dearth of evidence currently exists as to how such a strengthening method would change the response of a URM wall subject to a debris impact, particularly at velocities on the order of the requirements of FEMA-361. Schmidt and Cheng (2009) develop models to determine the impact resistance of URM walls strengthened with CFRP subject to a low velocity impact.

Two analytic models are based on energy principles and wave propagation theory, while a third model is developed using a finite element approach. An experimental verification is then performed using three 1.2m tall walls of 400mm thick CMU blocks. These walls, one strengthened with a continuous sheet of unidirectional CFRP, one strengthened with two layers

of woven CFRP, and one unstrengthened, were simply supported and loaded using a pendulum system impacting the wall at its center. The drop height of the pendulum was increased until the wall failed, indicated by cracking of the masonry. The results of these impact tests then allowed researchers to compare the validity of each model for determining the out of plane flexural strength of the new wall system subject to pendulum impact.

Figure 2.13 and Figure 2.14 below show the comparison of these models with the test results for the wall strengthened with a continuous unidirectional CFRP sheet and two layers of woven CFRP respectively. Due to the complexity of modeling masonry structures, experimenters concluded that the variation between theoretical and experimental results is reasonable. They also provide a qualitative assessment for each theoretical model. This comparison is shown in Table 2.6 shown below.

Table 2.6 Comparison of theoretical models for impact strength of CFRP strengthened masonry (Schmidt and Cheng, 2009)

Theoretical Method	**Advantages**	**Disadvantages**
Energy	-Simple and fast -Good estimates of maximum impact force and deflection	-No time history information
Wave Propagation	-Provides time history response	-Poor estimate of peak deflection -More complicated and time consuming
Finite Element Analysis	-Most accurate time history response -Good estimates of other maximum values	-Most time consuming and complex

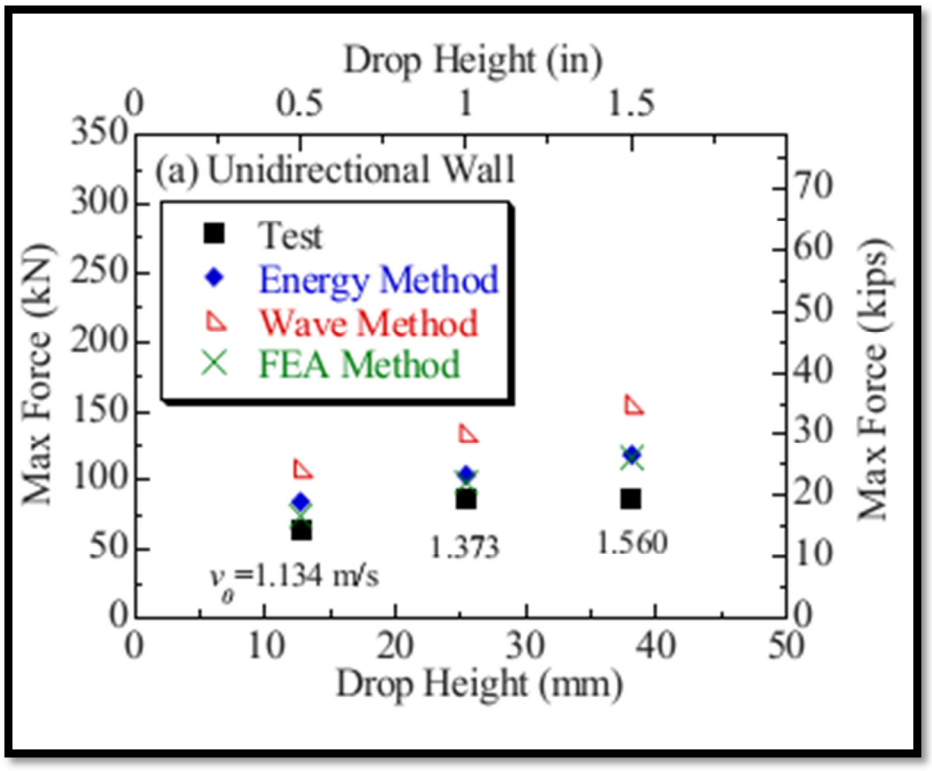

Figure 2.13 Comparison of theoretical models for impact strength of unidirectional wall (Schmidt and Cheng 2009)

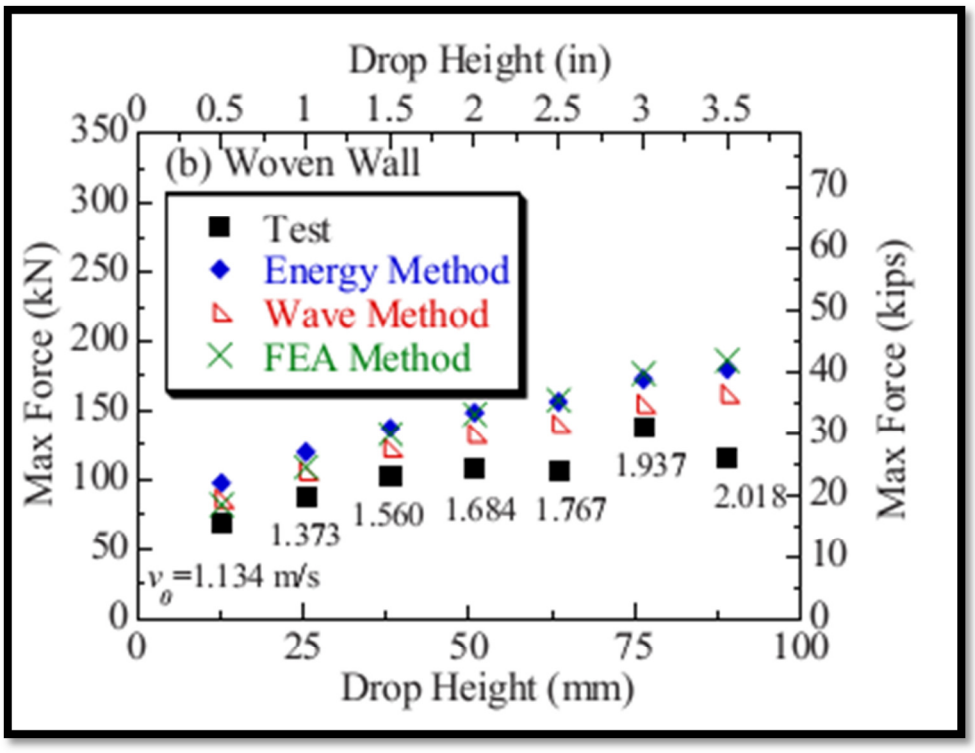

Figure 2.14 Comparison of theoretical models for impact strength of woven wall (Schmidt and Cheng 2009)

In these initial tests, moment capacity of the wall was determined using force equilibrium and an equivalent stress block, and the moment capacity found to be:

$$M_n = A_{frp} f_{fu} (h - 0.375 x_2) \quad (16)$$

with A_{frp} being the cross-sectional area of FRP reinforcement, f_{fu} its ultimate tensile strength, h the wall depth, and x_2 the neutral axis depth. Their walls were designed to meet the over-reinforced condition of flexural compression failure, finding that one layer of unidirectional FRP reinforcement increased the flexural capacity of the wall by 26%, and greatly improved impact response. By adding an additional layer of reinforcement, only small improvements were shown, leading researchers to conclude that walls need not be reinforced beyond the balance condition to successfully resist static flexural or dynamic impact loads.

As an extension of this same study, Cheng and McComb (2010) discuss the effect of CFRP layout. Using the same experimental setup and procedure, a total of nine walls were tested utilizing three distinct CFRP layouts on the back side of impact tested wall assemblies. The first set of walls contained an unreinforced control specimen, a wall reinforced with a unidirectional CFRP sheet, and one with two layers of continuous woven CFRP, applied in two layers so that it contained an equal number of fibers running in the vertical direction as the unidirectional wall. The second set of three walls tested reinforcement layouts of three, four, and five discrete vertical CFRP strips. All walls in this group had the same amount of woven CFRP as the continuous woven wall in the previous set. The last set of three walls contained the same amount of unidirectional fiber as the unidirectional sheet reinforced wall of the first group, but laid out in an orthogonal pattern, an orthogonal pattern with carbon fiber anchor bolts around the perimeter, and a diagonal pattern. Testing was performed until failure, which experimenters defined as either extreme masonry cracking or significant decrease in recorded impact force.

Based on experimental results, it was concluded that CFRP reinforcement can significantly increase the impact resistance of unreinforced concrete masonry walls. Furthermore, no premature CFRP delamination occurred, and all failure was due to masonry cracking.

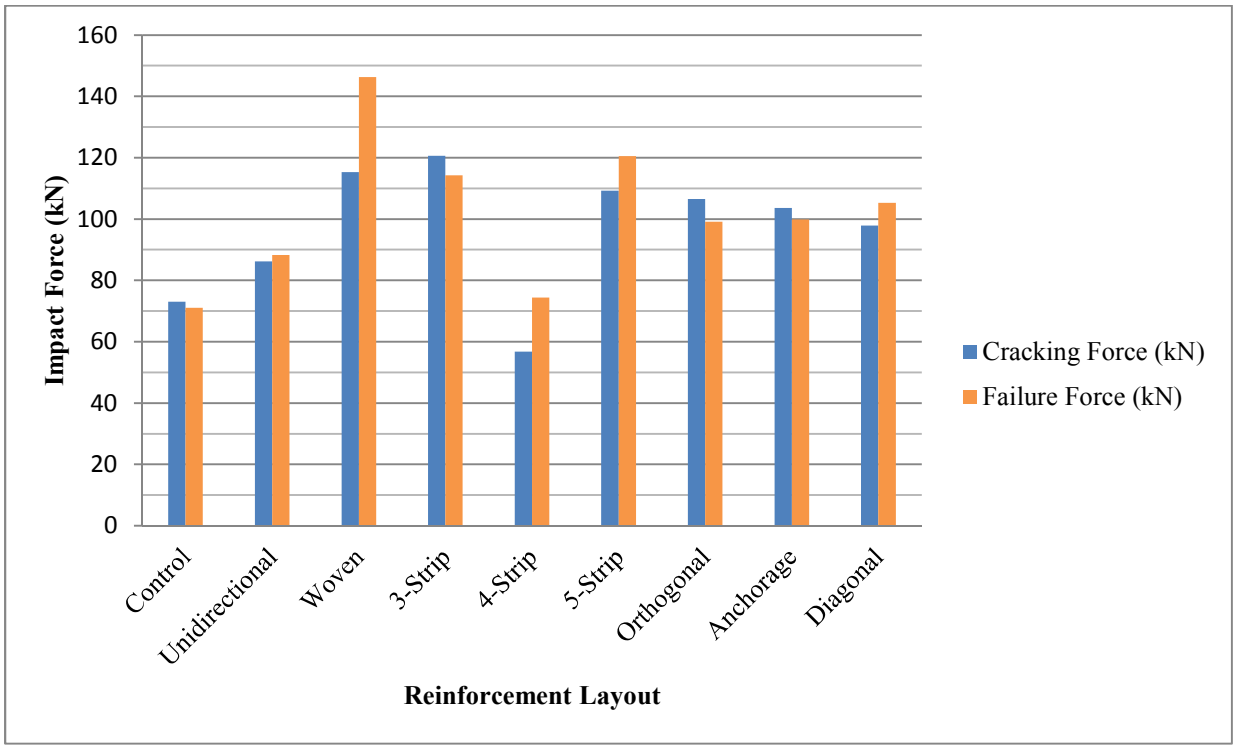

Figure 2.15 Comparison of impact forces for CFRP strengthened URM

Figure 2.15 compares the forces at which each experimental specimen showed first signs of cracking and ultimate failure. The woven, 3-strip, 5-strip, orthogonal, anchorage, and diagonal specimens all show similar forces at first cracking, while the 4-strip performs the worst. Experimenters conclude this is because the 3-strip and 5-strip provided reinforcement on the reverse side of the wall at the point of impact where the 4-strip did not, allowing for the formation vertical cracks at first impact. Thus, walls strengthened with vertical strips perform the best when at least one is directly behind the location of impact. The specimen with the

continuous woven CFRP sheet shows the greatest improvement when examining impact force at final failure.

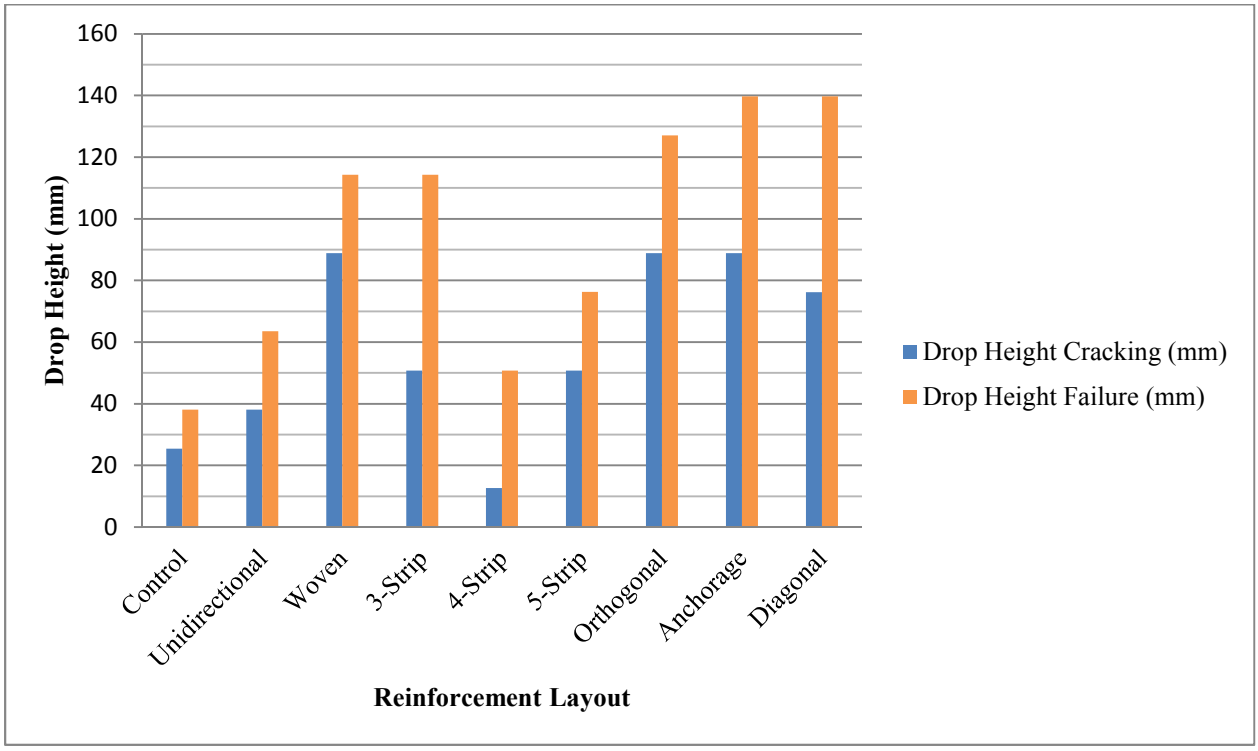

Figure 2.16 Comparison of drop heights for CFRP strengthened URM

Figure 2.16 again compares sign of first cracking and ultimate failure, but this time taking pendulum drop height as the dependent variable. From this perspective, the orthogonal, anchorage, and diagonal walls outperform others if concerned with final failure, while these three walls and the continuous woven wall provide the best results when the goal is to prevent cracking. Additionally, anchorage provides little improvement in the performance of the wall strengthened with orthogonally placed strips.

These two studies give support for the use of FRP to prevent premature cracking and failure in masonry walls. Preventing both conditions is important in the context of Tornado Safe Rooms because the goal of external walls is to protect occupants from flying debris and to remain uncompromised to prevent internal pressure changes which could lead to progressive

collapse. However, the velocity at which researchers performed their investigations precludes these studies from being directly applicable to Safe Room Design. Though the equations developed to predict maximum impact force are experimentally verified, the test procedure uses pendulum impact at a very low velocity, so it is unclear as whether the dynamic response of the FRP reinforced masonry wall will remain the same at higher velocities. Furthermore, the methods used to derive these equations assume that a negligible amount of energy is lost due to plastic deformation, and hence are only intended to predict maximum impact forces for low-velocity impacts.

2.5 Limitations of Current Research and Research Goals

The numerous studies investigating amount of FRP reinforcement, fiber type, bond surface preparation, and anchorage provide a reliable foundation for determining the effective application of FRPs to retrofit masonry walls to resist the extreme lateral pressure experienced by these wall assemblies in a tornado. Furthermore, the American Concrete Institute's publication of ACI 440.7R-10 provides engineers with a comprehensive guide for adding out-of-plane flexural reinforcement to URM giving guidance from design through construction. While it is well understood that structures with URM components are extremely susceptible to failure during extreme wind events, and that FRP represents a promising solution to mitigate the weaknesses that lead to such failures, the underlying motivation for most studies, and corresponding interpretation of results, remains centered on the use of FRPs in seismic applications (Velazquez-Dimas and Ehsani 2000).

Even though an understanding of the flexural response of FRP reinforced URM walls to lateral loads is important, it represents only the first half of what is necessary for a structure to be considered a "Safe Room" under FEMA-361. Contrary to the well-developed state of research on

increasing out-of-plane flexural strength, a dearth of studies investigates FRP retrofitting of URM to resist high velocity missile impacts. Current studies on the response of FRP strengthened URM only scratch the surface on how such complex, composite structural assemblies respond to dynamic impacts. With this in mind, it is safe to say that no studies explicitly determine the adequacy with which FRP can be used to fulfill the debris impact criteria of FEMA-361, despite the understanding that URM walls are extremely vulnerable to such impacts and represent one of the greatest threats to human safety in the built environment (Schmidt and Cheng 2009).

As a first step to filling in the gaps in the understanding of FRP reinforced masonry and its application to provide life safety in a tornado, a set of guidelines will be developed that attempt to satisfy both the lateral loading and debris impact criteria for Safe Rooms as required by FEMA-361.

This initial guide will propose to achieve two goals. The first simple, albeit important step is an explicit adaptation of the current guidelines for FRP reinforced URM to the first FEMA-361 protection objective of providing strength to resist wind forces. The second objective is to provide guidance for the application of FRP to URM walls in order to resist the high velocity impact of a tornado generated 15lb 2x4 timber. This objective is more complicated and will involve several assumptions and a reliance on accepted laws of mechanics to extrapolate what little experimental data exists on the impact resistance of FRP strengthened URM.

The following chapter provides a list of these assumptions and any significance or implication such an assumption may have on the resulting design guidelines. The design guidelines draw on both current design guides and research findings to provide a prescriptive method for meeting the wind force and debris impact protection requirements of FEMA-361.

This is followed by a discussion of the weaknesses and limitations of the new document, and areas where further research could help improve the accuracy and reliability of the newly created design guide.

Chapter 3 Guidelines for Strengthening URM Walls with FRP to Comply with the Requirements of a FEMA Safe Room

The economic and societal impacts of masonry collapse during extreme wind events such as tornadoes indicates an urgent need to provide an affordable and feasible method for reinforcing these structures against wind loads and debris impact. Current research indicates that Fiber Reinforced Polymers represent a promising choice for retrofitting of masonry structures, as its properties allow for a significant increase in flexural strength and impact resistance (Triantafillou 1998). However, while FEMA-361 adequately provides a method for determining loading conditions during tornadic events, it only accounts for conventional methods of reinforcement as a means to achieve the required strength to resist these loads. A review of literature, performed in sections 2.3 and 2.4, concerning FRP reinforcement of masonry indicates its adequacy for fulfilling the Tornado Safe Room requirements of FEMA-361; however, guidelines for increasing flexural strength need to be applied and adapted to fulfill FEMA requirements, and no guidelines exist for FRP strengthening of masonry against high-velocity impacts.

This chapter aims to address these two limitations, the final result being a design guide that allows an engineer to retrofit masonry walls with FRP such that they fulfill the flexural strength and debris impact requirements of FEMA-361. The first section lists the assumptions made, and what implications they will have on the final design guidelines. Next, information derived from these assumptions is assimilated with evidence provided by current research to fill the gaps between experimental findings and practical design for Tornado Safe Rooms. This section also shows how design equations are derived, giving corresponding explanations for the current research and assumptions on which they rely. Last, these equations are presented as a

comprehensive set of design guidelines which provide engineers with a means of using FRP to retrofit masonry walls so that they fulfill the requirements of a FEMA Tornado Safe Room.

3.1 Assumptions and Related Implications

The masonry wall should be considered part of a Residential Stand Alone Safe Room

FEMA-361 divides its Safe Rooms into two categories based on occupancy: Residential Safe Rooms designed for the occupancy of sixteen or fewer persons, and Community Safe Rooms which are designed with capacities from sixteen to several hundred. Addressing Tornado Safe Room design, the document states, "The design methodology used for residential safe rooms is the same as for tornado community safe rooms." The only difference is in the selection of design wind speeds; design wind speeds for Community Safe Rooms are based on the Tornado Safe Room Design Wind Speed Map (Figure 2.2) and range from 130 to 250 mph, while Residential Safe Rooms default to the highest wind-speed zone of 250 mph. For the design of a wall assembly, building capacity is irrelevant; however, the structure will be assumed to be part of a Residential Safe Room in order to ensure use of the highest design wind speed.

FEMA-361 also differentiates between "Stand-Alone Safe Rooms" and "Internal Safe Rooms" which may be part of a larger structure. For the purposes of this investigation, wall assemblies will be considered as part of a Stand-Alone Safe Room, as such structures experience the full force of debris impact and wind loading. This does not preclude the applicability of the design guidelines for internal safe rooms, as walls of internal safe rooms will generally be treated as Components and Cladding for determination of wind loads.

The design wind speed is taken as V_x=250mph (FEMA-361 3.5.1)

This is the highest wind design category and represents the upper end of EF5 tornado wind speeds. With an annual probability of .000001, assuming this wind speed zone provides a conservative estimate for even the riskiest regions.

The 15-lb 2x4 timber for impacts vertical wall surface at 100mph

This impact speed used in the safe room missile impact criteria corresponds to the 250mph design wind speed as per FEMA-361, Tbl. 3-6. Protecting inhabitants from tornado generate debris is extremely important in safe room design, and this criterion can control when designing smaller safe rooms.

The wall is to be considered part of the MWFRS

As per ASCE-7, Method 2, for determining wind loads, structural components may be classified as either part of the Main Wind Force Resisting System (MWFRS) or Components and Cladding (C&C). This classification does not depend on the type or reinforcement of the wall, but rather the way in which it transmits loads. FEMA-361 dictates elements experiencing axial, shear, and bending loads, or only axial and shear, shall be classified as part of the MWFRS, while elements subject to axial and bending loads only shall be considered part of the MWFRS for determination of Axial loads and C&C for determination of bending loads. Following from the first assumption, the wall is part of a stand-alone structure experiencing the full force of all loading. As such, the walls designed are subject to the former condition and shall be considered as part of the MWFRS.

The wall geometry is dictated by FEMA-361

The maximum allowable wall span is 14ft as per FEMA-361, chapter 7. Safe room height is limited to 8ft of vertical wall as per FEMA-361 Chapter 3, Section 5.1. Use of these maximum

wall dimensions also places the walls considered well within the empirical height-to-thickness ratio design rules observed by many designers, 20 for fully grouted load bearing walls and 18 for other load bearing walls (ACI 530-08 2007).

Carbon, glass, and aramid fibers may be used

The efficiency of fiber reinforcement is dictated by its unidirectional tensile strength. In general, carbon and aramid fibers are much stronger than glass. The choice of fiber can vary considering both strength and cost considerations, and taking the ultimate tensile strength "f_{fu}*" and ultimate rupture strain "ε_{fu}*" as provided by the manufacturer. However, preference should be given to fibers which allow for fulfilling the over-reinforced condition with application of only a single layer of FRP. A single layer application is preferred to ensure development of adequate bond strength and consistent wall behavior, and because very little impact resistance improvement is shown beyond a single layer of enforcement (Schmidt and Cheng 2009).

The wall should be reinforced to the over-reinforced condition ($\rho > \rho_{fb}$)

Conventional design, i.e. the design of reinforced concrete, calls for under-reinforcement. In the case of steel-reinforced concrete, this ensures that the reinforcement steel will experience tension yielding before the masonry experiences crushing failure, and because steel yielding contains a significant plastic zone before rupture, this provides inhabitants of these structures with considerable warning as to their failure allowing for evacuation, demolition, and or structural rehabilitation. However, the using FRP to reinforce URM to resist tornadic loading provides several distinctions leading to a deviation from conventional design practice.

First, the mechanical behavior of FRP differs from that of other reinforcing materials. Unlike steel which enters a zone of plastic deformation prior to rupture, FRPs behave linearly elastic until failure. Tensile rupture of FRP is sudden, and without warning and thus provides no

better indication of failure than the masonry crushing failure mode (Velazquez-Dimas and Ehsani 2000). Second, the goal of a storm shelter is much different than a conventional structure. A typical building is designed considering a combination of strength and serviceability conditions; the structure provides a certain level of performance under expected use, and any unforeseen circumstance or accidental loading should lead to a mode of failure which allows inhabitants enough time to safely evacuate. A storm shelter, however, is designed with life-safety as its only concern. Providing an advanced warning of structural failure is of little use to the inhabitants who refuge in the shelter as a last resort, with evacuation being impossible. Therefore, designing for strength will be the dominate design paradigm considered resulting in over reinforcing the masonry walls.

For the case of FRP reinforced masonry, ρ_{fb} is the ratio of FRP reinforcement to masonry surface area at which masonry crushing occurs simultaneously with FRP rupture. In an attempt to provide an upper bound on this reinforcement condition and keep the design guidelines within the realm of practicality, a maximum reinforcement ratio of $2\rho_{fb}$ will be set. This provides a way to fulfill the reinforcement objective while still keeping the design practical and economical. Furthermore, experimental evidence indicates that beyond this reinforcement ratio the wall will develop little capacity and transition out of the desired masonry crushing failure mode (Velazquez-Dimas and Ehsani 2000).

The surface of the masonry should be prepared prior to FRP bonding

In determining the failure mode, the amount of reinforcement used is irrelevant if one cannot ensure a proper bond between the surface of the masonry and the FRP (Velazquez-Dimas and Ehsani 2000). As such, all CMU surfaces to be externally strengthened shall be prepared by either sandblasting or wire-brushing, cleaned, and allowed to dry prior to application of the

bonding epoxy. Furthermore, presence of even a thin layer of plaster or other finish to the masonry dramatically decreases the flexural capacity of the FRP reinforced URM wall by facilitating debonding at either the masonry/plaster or plaster/FRP interface (Camli and Binici 2007). As such, anchor embedment and will be a requirement for all walls with a plaster or other finish.

Energy is assumed to be conserved when determining the nominal impact strength

Perhaps the greatest assumption involves how evaluate the resistance of FRP reinforced URM walls against debris impact. Because it provides a relatively accurate and straight-forward way to determine the ultimate impact force capable of being sustained by an FRP reinforced URM wall, the energy method used by Schmidt and Cheng (2009) will be modified for the purpose of designing a wall to resist a high-velocity impact. This relies on the Hertz Contact Law which takes the kinetic energy of the projectile immediately before impact equal to strain energy stored in the wall after impact. Relying on this method to determine impact strength of the wall in Tornado Safe Room design is valid for two reasons; first, experimental verification determines that implementation of the Hertz Contact Law, which assumes that the kinetic energy of the debris immediately before impact is converted to strain energy and stored in the wall being impacted, leads to a successful prediction of maximum contact force (Cheng and McComb 2010). Second, due to the relative stiffness of the timber and masonry wall, significant deformation of the timber is likely to occur, leading to a loss of energy not accounted for by the Hertzian Contact Law. This energy loss associated with higher impact velocities will lead to an underestimation of the impact strength of a FRP strengthened masonry wall, leading to a conservative formulation of nominal impact strength.

The impact of the missile is considered elastic when determining the ultimate impact force

In a perfectly plastic impact, the force of the timber on the masonry wall would equal the momentum of the timber missile as the two colliding bodies stick together. In an actual collision scenario, this would manifest as the timber embedding into the masonry wall, as only a small amount of energy is lost in the local crushing of the masonry. Therefore, the impact between the wall and the timber is assumed to be perfectly elastic, hence the impact force is two times the missile's momentum as the rebound velocity of the timber equals its initial velocity. This will lead to an overestimation of the ultimate impact force experienced by the wall, as the collision is neither perfectly elastic nor plastic; however, impact testing for Southern Yellow Pine 2x4 members at various impact speeds indicates that at high missile velocities, the impact response becomes more elastic (FEMA P-361 2008).

The fiber should be laid out as orthogonal or diagonal patterns of discrete strips or a continuous woven sheet

Experimental evidence indicates that while fiber layout has some effect on increasing flexural strength, the amount of reinforcement (aligned vertically) and development of adequate bond strength are much more important. Given these two conditions are satisfied, it is unlikely that the layout chosen for FRP reinforcement will significantly impact the wall's flexural strength.

The limiting condition in this case is providing for impact resistance. The absence of FRP reinforcement immediately behind the point of impact greatly decreases the force at which the wall experiences first cracking and ultimate failure (Cheng and McComb 2010). When considering both flexural and impact requirements, in addition to providing adequate fiber in the vertical direction to exceed the balance condition, as much of the surface of the wall should be covered in order to provide impact resistance. Therefore, FRP reinforcement should be applied

as either a continuous woven sheet or as unidirectional strips applied in an orthogonal or diagonal grid, as this layout best strengthens the wall, see Figure 2.16.

Both sides of the wall should be reinforced

In regards to hollow masonry construction, design guidance recommends reinforcing on one face of wall for 8in and smaller units un-grouted or with grouted cells spaced greater than 48in., and reinforcing on both faces in most other circumstances (ACI 440.7R-10 2010). Reinforcement on both sides of the wall is shown to increase the bending capacity of the assembly, though this is still limited by the assumed mode of failure (Tan and Patoary 2004). Because the walls of storm shelters must withstand both inward (positive) pressures acting at windward surfaces and negative (outward) pressures acting at leeward and side surfaces, equal amounts of reinforcement shall be provided on the interior and exterior surfaces of exterior walls for all partially grouted and un-grouted walls of 12in units or smaller.

3.3 Derivation of Design Guidelines

The above assumptions will be utilized to derive design guidelines for the strengthening of masonry walls with Fiber Reinforced Polymer (FRP) composites to resist two loading conditions; out-of-plane wind loading and high-velocity debris impact. Hence, the design guidelines are broken into three components, the first detailing how to reinforce the masonry wall to add flexural strength, the second explaining how to provide debris impact resistance, and the third discussing the interaction between reinforcing requirements for the two conditions The aim of this section is to describe how current research and literature aid in the creation of these new guidelines for FRP strengthening of concrete masonry to resist tornado loading, where current research is inadequate in explicit guidance for Tornado Safe Room design, and how the assumptions made above allow for bridging this grip to create a final set of design guidelines.

Flexural Strength

Section 2.1 explains that the strength of FEMA-361 is it allows for accurate determination the loading conditions experienced by a Safe Room during an extreme wind event. FEMA-361 provides designers with a modified set of design coefficients for use with Chapter 6, Method 2 of ASCE 7, "Analytical Procedure for Wind Loads." The design procedure is quite clear, with the only ambiguity stemming from the determination of the External Pressure Coefficient C_p and/or Force Coefficient C_f. These coefficients are used to determine the pressure acting on the wall, and require that the wall be classified as either part of the Main Wind Force Resisting System (MWFRS), which receive tributary loads from other structural components, or as Components and Cladding (C&C) which is classified as a part of the building envelope that does not qualify as part of the MWFRS (ASCE 7-05 2005). In general, Stand-Alone Safe Rooms will be load bearing, receiving tributary loading from the concrete roof slab as well as in-plane loads from the side walls; therefore, most walls of Stand-Alone Safe Rooms are part of the MWFRS. The first assumption above assumes the Safe Room being designed is stand alone, hence is load bearing and should be considered as part of the MWFRS.

After determining the loads which act on the masonry wall, the existing strength must be assessed. Though the review of case studies of masonry performance in tornadoes indicates that the tensile strength of masonry is inadequate, the current strength of the wall should be computed. To compute the tensile stress of the wall, one must consider the tensile stress as a result of out-of-plane bending minus the pre-stressing of the wall provided from axial load. Expressing this as an equation, additional reinforcement is required if:

$$f_b > \phi f_r \tag{17}$$

where

$$f_b = \frac{M_u}{S} - \frac{P_u}{A_n} \tag{18}$$

and f_b is the compressive stress in the masonry due to bending, M_u is the ultimate factored moment, S is the Section Modulus of the Masonry, P_u is the ultimate factored axial load, and A_n is the net area of mortared section.

Knowing the design load and that additional flexural reinforcement is needed, the provisions of ACI-440.7R-10 shall be used to determine the required amount of FRP reinforcement. From the assumptions above, the wall is to be reinforced such that the reinforcement ratio ρ is greater than the balanced condition ρ_b. When determining the depth of the neutral axis, this assumption allows the parameters γ and β_1 to be taken equal to 0.80 (see Figure 2.12). This allows the neutral axis location, c, to be iteratively determined from ACI 440.7R-10, Eq. 9-3:

$$\varepsilon_m = \varepsilon_{fe}\left(\frac{t-c}{c}\right) = \varepsilon_{mu} \tag{19}$$

Where ε_m is the strain experienced by the masonry, ε_{mu} is the maximum masonry strain taken as .0025, t is the thickness of the wall, and ε_{fe} is the effective strain in the reinforcement found by taking the ultimate rupture strain, ε_{fu}*, as reported by the manufacturer multiplied by an environmental reduction factor found in ACI 440.7R-10, Tbl. 8.1. The required area of reinforcement can then be found using force equilibrium:

$$A_{f\_req} = \frac{\gamma \cdot f'_m \cdot \beta_1 \cdot c - P_u}{f_{fe}} \tag{20}$$

Where f_{fe} is the effective stress level in the reinforcement found by taking the effective strain in the reinforcement, ε_{fe}, multiplied by the FRP modulus of elasticity E_f, where ε_{fe} is equal to the ultimate rupture strain provided by the manufacturer, ε_{fe}*, times a bond dependent coefficient for flexure κ_m found in ACI 440.7R-10, Eq. 8-8).

However, because we have assumed the masonry crushing failure mode, as an alternative to the procedure in ACI 440.7R-10 the required reinforcement ratio can be determined directly from computing the balanced reinforcement ratio:

$$\rho_{fb} = (\frac{f'_m}{f_{fe}})(\gamma \cdot \beta_1 \left(\frac{\varepsilon_{mu}}{\varepsilon_{mu}+\varepsilon_{fe}}\right) - \frac{P_u \cdot b}{b \cdot t \cdot f'_m}) \quad (21)$$

Where f'_m is the compressive stress in the masonry. The minimum reinforcement area, A_{f_req} can then be found by multiplying ρ times the area of the wall to be reinforced.

Now that a lower bounds on reinforcement has been established, A_{f_req}, an upper bounds will be set as well. Velazquez-Dimas and Ehsani (2001) indicate that reinforcing beyond $2\rho_{fb}$ adds little to flexural strength as the wall becomes likely to fail in shear rather than masonry crushing. Therefore, the upper bounds on reinforcement shall be set at two times the balanced condition.

Debris Impact Resistance

The requirements for a FEMA Residential Tornado Safe Room require that walls of a tornado safe room be able to prevent perforation by a 15lb 2x4 timber traveling at 100mph. While FEMA-361 provides cross-sections of steel-reinforced masonry and other common construction materials which meet this requirement, it provides no way to determine the load created by this debris impact, hence no way to determine the adequacy of alternative cross-sections short of a full-scale impact test. In order to bypass such a dubious undertaking, the ninth assumption above outlines that the response of the wall under a high velocity impact will be taken that describe by the Hertz Contact Law, outlined by Schmidt and Cheng (2009), assuming conservation of Kinetic Energy. The Hertz Contact Law states that:

$$F_{impact} = Kz^{\frac{3}{2}} \quad (22)$$

where z is the indentation and

$$K = \frac{4R_s^{\frac{1}{2}}\left[\frac{1-v_s^2}{E_{st}}+\frac{1}{E_m}\right]^{-1}}{3} \tag{23}$$

R_s, υ_s, and E_{st}=radius, Poisson's ratio, and Young's modulus for the indentor, which in the case of Schmidt and Cheng (2009) was a steel sphere.

Schmidt and Cheng (2009) also use an energy balance equation which states that the combined energy stored in bending, shear, membrane stretching, and local indentation of a body after impact by an indentor is equal to the kinetic energy of that indentor immediately prior to impact. In equation form this is represented as:

$$\frac{1}{2}m_1 v_0^2 = E_b + E_s + E_m + E_c \tag{24}$$

Substituting for various Energy terms and combining Eq.'s 17 and 18 led to a formula for determining the maximum impact force of a wall assembly:

$$\frac{1}{2}m_1 v_0^2 = \left(\frac{1}{2}\right)\left(\frac{F_n^2}{k_{eq}}\right) + \left(\frac{2}{5}\right)\left(\frac{F_n^{\frac{5}{3}}}{K^{\frac{2}{3}}}\right) \tag{25}$$

where

$$K = \frac{5in^{\frac{1}{2}}}{3}\left[\frac{1-v_w^2}{E_w}+\frac{1}{E_m}\right]^{-1/3} \tag{26}$$

$$k_{eq} = \frac{F_{impact}}{w_{max}} = \frac{1}{(0.02304)\frac{lh}{D}} \tag{27}$$

and k_{eq} is the equivalent bending stiffness of the wall, F_{impact} is the ultimate impact force described, E_w and E_m are the Young's Modulus of wood and masonry, υ_w is Poisson's Ratio of wood, lh represents the area of the wall elevation, and D the specific flexural rigidity of the reinforced wall. A more detailed derivation of these formulas is found in the Appendix.

This result for nominal impact strength must be compared to an ultimate impact force experienced by a wall under debris impact. Assuming conservation of momentum, the dynamic

impact force is equal to the impulse of the impacting body divided by the impact duration. This yields:

$$F_{impact} = \frac{WV}{gT} \tag{28}$$

Where W is the weight of the missile, V is its velocity, g is acceleration due to gravity, and T is impact duration. Typical durations of impact for tornado debris are on the order of 1-2 milliseconds (FEMA P-361 2008). However, because the impact is not perfectly inelastic (this assumes the condition that the missile embeds in the wall, which is the situation trying to be avoided), a conservative scenario where the impact force is equal to two times the impact momentum shall be considered such that:

$$F_{impact} = \frac{2WV}{gT} \tag{29}$$

Assuming the collision is perfectly elastic is a conservative estimate considering we know some energy will be lost in the deformation of the timber; however, we also know that because our design criteria aims to prevent perforation of the wall by the timber, the impact will not be perfectly plastic either. In reality, the impact is classified somewhere in between elastic and plastic.

Finally, the requirement for impact strength is expressed as:

$$\phi F_n \leq F_{impact} \tag{30}$$

The strength-reduction factor ϕ can presumably be any decimal value to increase the conservative nature of the design. Considering bending, shear, bearing, and flexure, perforation of a masonry wall most closely resembles a punching shear failure. As such, the value of ϕ shall be taken as 0.80 as with other masonry designed to resist shear forces (ACI 530-08 2007).

Combined Flexural Strength and Debris Impact Resistance

No literature specifically addresses reinforcing masonry walls to resist high-speed velocity impacts and significant out-of-plane bending forces; hence, this final section is needed to consider the interaction between the two sets of requirements. Initial evidence indicates that providing reinforcement beyond the balanced condition for flexural strength does little to increase flexural capacity or impact strength (Schmidt and Cheng 2009). However, the wall should be designed for flexure and checked to ensure adequate impact strength is available. If this second condition is not satisfied, the area of reinforcement shall be increased until adequate impact strength is obtained.

The only significant difference between reinforcing masonry walls for flexural versus impact strength deals with the reinforcement layout. Experiments testing walls in bending found that the single most important variable is the FRP/masonry bond strength (Hamilton and Dolan 2001). If this bond is adequate, the layout of the fibers has little effect on overall behavior for a given reinforcement condition, either over or under-reinforced (Albert, Elwi and Cheng 2001). Conversely, investigations into reinforcing for impact strength point towards use of diagonal or orthogonal grids of unidirectional FRP strips or a sheet of continuous woven FRP reinforcement. These layouts performed better because walls were much more susceptible to cracking if there was no reinforcement directly behind the point of impact, as was the case for unidirectional reinforcement laid out in discrete, vertical strips (Cheng and McComb 2010). When designing a Tornado Safe Room, the location of debris impact is unknown, hence, reinforcement patterns that provide the most coverage are preferred. This indicates that continuous woven sheets, vertical strips in a diagonal pattern, and vertical strips in an orthogonal pattern are the preferred reinforcement layouts.

3.2 Design Guidelines

1. Flexural Strength

1.1. *Scope*—This section provides guidelines for increasing the out-of-plane bending strength of masonry walls to resist pressure induced by an extreme wind event

1.2. *Determination of Wind Load*—Lateral wind load on wall assembly shall be calculated according to ASCE 7-05, Chapter 6, Section 6.5,

Method 2-Analytical Procedure assuming the following constants:

a) Design Wind Speed: V_x=250 mph

The Design Wind Speed shall be taken as 250 mph which represents the upper end of wind speeds experienced during category EF5 tornadoes.

b) Importance Factor: I=1.0

Because annual probability of exceedence for the 250mph wind event is very low, no need to adjust using an Importance Factor greater than 1.

c) Exposure Category: C

Safe Rooms shall be considered to be located in open terrain as extreme wind events will raze surrounding buildings and trees.

d) Directionality Factor: K_d=1.0

K_d accounts for the tendency of tornadic winds to change direction, thus shall not be taken as less than 1.0.

e) Topographic Effects: $K_{zt} \leq 1.0$

Safe rooms should not be placed where they are likely to experience topographic effects, hence, K_{zt} need not be taken greater than 1.

f) Gust Effect Factor: G=0.85

The gust factor accounts for wind turbulence and is taken as equal to 0.85 as permitted by ASCE 7-05.

g) Enclosure Classification: Partially Enclosed

The amount of openings in a building's envelope determines its enclosure classification, but Tornado Safe Rooms shall be considered Partially Enclosed to account for the effects of Atmospheric Pressure Change (APC) associated with a tornado.

h) Internal Pressure Coefficient: $GC_{pi}=\pm 0.55$

Accounting for atmospheric pressure change, designing for $GC_{pi}=\pm 0.55$ eliminates the need to provide venting in the building

i) External Pressure Coefficients C_p or Force Coefficients C_f

These coefficients are based on the physical dimensions and shape of the structure and shall be determined as per ASCE 7-05 Section 11.5.2.2 and 11.5.2.3

Use MWFRS designation for walls experiencing:

- Axial, Shear, and Bending
- Only Axial and Shear

Use Components and Cladding (C&C) and Main Wind Force Resisting System (MWFRS) designations for walls experiencing only axial and bending forces as follows:

- MWFRS for Axial
- C&C for Bending

1.3. *Existing CMU tensile Strength*—Determine existing tensile strength of masonry wall to determine if additional strengthening is needed

1.3.1. Existing tensile strength f_r shall be determined from ACI530-08, Tbl. 2.2.3.2

1.3.2. Maximum tensile stress shall be computed as:

$$f_b = \frac{M_u}{S} - \frac{P_u}{A_n} \quad \text{(Eq. G-1-1)}$$

1.3.3. If:

$$f_b > \phi f_r \quad \text{(Eq. G-1-2)}$$

Where $\phi = 0.60$, additional reinforcement is required

1.4. *FRP Reinforcement*

1.4.1. Use ACI-440.7R-10 to determine required amount of FRP reinforcement using the following assumptions:

a) Crushing of masonry is controlling failure mode. For equivalent rectangular stress block this implies:

$$\gamma=0.80 \quad \text{(Eq. G-1-3)}$$

$$\beta_1=0.80 \quad \text{(Eq. G-1-4)}$$

b) *Fiber Type*-Reinforcement Fiber Type shall be such that controlling failure mode can be obtained using a single layer of FRP reinforcement

1.4.2. Alternatively, the required are of reinforcement can be determined directly from the balanced reinforcement ratio as:

$$A_{f\_req} = \rho_{fb} bt \quad \text{(Eq. G-1-5)}$$

where

$$\rho_{fb} = \frac{f'_m}{f_{fe}} \left(\gamma\beta \left(\frac{\varepsilon_{mu}}{\varepsilon_{mu}+\varepsilon_{fe}}\right) - \frac{P_u b}{b t f'_m}\right) \quad \text{(Eq. G-1-6)}$$

The location of the neutral axis can then be found using an equivalent rectangular stress block:

$$c = \frac{A_{freq} f_{fe} + P_u b}{\gamma f'_m \beta_1 b} \quad \text{(Eq. G-1-7)}$$

1.4.3. *Limiting Reinforcement Ratio*—The area of reinforcement provided in the vertical direction shall be less than or equal to two times the required area to achieve the masonry crushing failure mode

$$\rho_{fb} < \rho \leq 2\rho_{fb} \quad \text{(Eq. G-1-8)}$$

2. **Debris Impact Resistance**

2.1. *Scope*—This section shall provide guidance to determine the required reinforcement to resist impact of 15lb 2x4 wooden board member

2.2. *Allowable Forces*—For CMU walls reinforced Fiber Reinforced Polymers shall provide enough impact resistance such that:

$$\phi F_n \geq F_{impact} \quad \text{(Eq. G-2-1)}$$

where ϕ=0.80

2.3. *Maximum Impact Force*—The force of the timber striking the wall shall be calculated as:

$$F_{impact} = \frac{2(m_w)(v_0)}{T_i} \quad \text{(Eq. G-2-2)}$$

Where m_w=mass of wood missile (15lb), v_0=impact velocity (100mph=147ft/sec), and T_i=impact duration (~$1x10^{-3}$ sec)

2.4. *Nominal Impact Strength*—Nominal impact strength (F_n) of the wall assembly against the representative timber missile shall be calculated iteratively using:

$$\frac{1}{2} m_1 v_0^2 = \left(\frac{1}{2}\right)\left(\frac{F_n^2}{k_{eq}}\right) + \left(\frac{2}{5}\right)\left(\frac{F_n^{\frac{5}{3}}}{K^{\frac{2}{3}}}\right) \quad \text{(Eq. G-2-3)}$$

where

$$K = \frac{5in^{\frac{1}{2}}}{3}\left[\frac{1-v_w^2}{E_w} + \frac{1}{E_m}\right]^{-1/3} \quad \text{(Eq. G-2-4)}$$

and

$$k_{eq} = \frac{F_{impact}}{w_{max}} = \frac{1}{(0.02304)\frac{lh}{D}} \quad \text{(Eq. G-2-5)}$$

where v_0 =Impact Velocity (100 mph), m_l=mass of missile (15lb), E_m=Young's Modulus of CMU, b=width of CMU wall, h=height of CMU wall, D=specific flexural rigidity of composite wall, υ_w=Poisson's Ratio of wood missile, and E_w=Young's Modulus of wood missile.

3. **Combined Flexural Strength and Debris Impact Resistance**

3.1. Amount of Reinforcement—The amount of fiber running in the vertical direction shall satisfy sections *1.4.1* and *2.2*

3.2. Enforcement Layout—Section 3.1 shall be satisfied using one of the following conditions:

a) Unidirectional Strips

b) Continuous Woven Fabric

c) Diagonal Strips

for conditions (a) and (c), and equal amount of fiber reinforcement shall be provided orthogonal to the placement of fiber used to satisfy *3.1*

Chapter 4 Application and Discussion of Proposed Guidelines

4.1 Contribution

Both the literature review and original design document presented above contribute to the current body of research regarding the application of Fiber Reinforced Polymers to Un-Reinforced Masonry Walls. First, the literature review points out the neglect of the engineering and construction industries in addressing the inadequacies of current design procedures for concrete masonry, especially in un-reinforced or under-reinforced conditions. A combination of high stiffness and low compressive pre-stressing makes such structures extremely susceptible to failure during an extreme wind event (Sparks, Liu and Saffir 1989). This represents not only the greatest risk to life-safety of any structural system, but also a billion dollar investment to properly strengthen these walls using the expensive and labor-intensive approaches associated with conventional reinforcement (Schmidt and Cheng 2009).

Identifying the inadequacies of URM in extreme wind events, a potential solution is found in the external application of Fiber Reinforced Polymers, with particular attention given to the possibility of using these composites to satisfy design guidelines for storm shelters which represent the last hope for safety and protection for many residents of tornado prone areas. Currently, guidelines exist for evaluating a current structure for its adequacy as a tornado shelter according to the requirements set forth in FEMA-361, and even go as far as to recommend the possible use of using fiber-reinforced materials to add flexural strength to masonry walls (Coulbourne, Tezak and McAllister 2002). However, any sort of guidance on how the plethora of choices of FRP reinforcement can be used to increase the bending strength and impact resistance of a CMU wall as part of a storm shelter or safe room is notably lacking.

This represents the next contribution; an investigation of studies on the various mechanical properties of composite FRP/masonry systems to determine if and how these laminates can be used to satisfy the stringent design requirements for Storm Shelters sanctioned by FEMA-361. By amalgamating current research investigating the variables of amount of fiber, fiber type, fiber layout, surface preparation, and FRP anchorage it is discovered that beyond its use for design level wind events, FRP reinforcement represents a viable option for strengthening un-reinforced masonry walls against lateral loads associated with tornados. It is shown that the current guidelines published by ACI can be easily adapted to fulfill the requirements for flexural strength dictated by FEMA-361. Additionally, evidence is discussed pointing to FRP as a solution to increase the missile resistance of masonry walls. Though research is limited, current experimental data is extrapolated to create preliminary equations for using FRP to increase the impact resistance of masonry walls, and to prevent perforation or cracking after the impact of a 15lb 2x4 timber at 100mph. Additionally, preliminary results indicate that by providing a URM wall with enough FRP reinforcement to fail in masonry crushing, significant impact resistance is added in addition to the marked improvement in flexural strength.

The evidence supporting the application of FRP to fulfill the two design requirements of FEMA-361 are then combined to create an original document, a preliminary design guide for use of FRP to reinforce the masonry walls of FEMA Tornado Safe Rooms. Though several extrapolations are used, the assumptions made are conservative and thus lead to what is likely an upper bound for the design of FRP reinforced masonry walls.

Presented now is a design example which utilizes the guidelines developed in Chapter 3 to design FRP reinforcement to retrofit an existing masonry wall. As per the assumptions of Chapter 3 of this document, the wall considered is to be reinforced such that it meets the

requirements of a Stand-Alone Residential Tornado Safe Room. As a part of a Stand-Alone Safe Room, the wall being considered is part of the MWFRS, and carries axial load from the roof slab, taken as 300 pounds per linear foot. The wall is single wythe and is composed of 10" units bonded using type N mortar, typical of U.S. masonry construction. In addition to being unreinforced, the wall considered is un-grouted to illustrate retrofitting of a worst case condition.

The design calculations follow the guidelines presented in Chapter 3 of this document. First, the wind load is determined using ASCE 7-05 Chapter 6, Section 6.5, Method 2, using the coefficients of Section 1.2. Once the load is determined, the ultimate moment and required nominal flexural moment is be determined and used to find whether additional reinforcement is needed as per Eq. 1-1 and 1-2. When it is determined that additional reinforcement is needed FRP reinforcement is designed according to Section 1.4. Aslan400 Carbon Fiber Laminate is chosen as the FRP material here, though any glass, aramid, or carbon fiber can be selected provided the manufacturer provides the tensile and modulus properties, and that these were obtained in accordance with the American Society for Testing and Materials (ASTM) "Standard Test Method for Tensile Properties of Polymer Matrix Composite Materials." The properties of Aslan4000 CFRP are shown in Figure 4.1. Both the design procedure in Section 1.4.1 which dictates the iterative method of ACI-440.7R-10 and the alternative procedure of Section 1.2 are used to determine the required reinforcement area, A_{f_req}, to show that both methods are equivalent. A reinforcement layout is chosen as 4" discrete vertical strips spaced every 12" on center. This layout is checked to determine that it both exceeds the required reinforcement ratio, but is less than two times the required ratio, as per Section 1.4.3, Eq. 1-9.

Next, the reinforcement required for impact strength is determined using Section 2. Eq.'s 2-3 through 2-5 are used to find the nominal impact strength of the wall, using properties of

Subalpine Fur for the 2x4 wood missile. The flexural rigidity of the wall is found by adding the contribution of the FRP reinforcement selected to the FRP to the bending stiffness. Once the impact force is found iteratively using Eq. 2-3, the Nominal Impact Force is compared to the maximum impact force found using Eq. 2-2. It is found that the reinforcement selected for flexural strength provides adequate impact resistance.

Finally, the reinforcement considerations for flexural strength and impact resistance are addressed as per Section 3. Adequate flexural strength has been designed in the vertical direction, so no more reinforcement need be added; however, the same FRP width and spacing will be placed running in the horizontal direction to create an orthogonal grid, Section 3.2, as this provides the best impact resistance. Because walls experience both positive and negative pressures, this final reinforcement scheme will be provided on both sides of the wall. The final reinforcement layout is shown in Figure 4.2.

Design Example

This design example examines the task of designing Fiber Reinforced Polymer reinforcement to retrofit an unreinforced masonry wall that is part of a Stand-Alone Residential Tornado Safe Room, as per FEMA-361. As such, this wall must resist the load of 250mph winds and the impact of a 2x4 timber traveling at 100mph. As a stand-alone structure, the wall being designed will support its own weight and the weight of the concrete roof slab. This total factored axial load equals 300 pounds per linear foot. The wall is composed of 10" concrete masonry units and is un-grouted with no steel reinforcement. The courses of masonry are bonded using type N mortar.

The properties of the CMU used in the example are:

$P_u := 300 \ \frac{lbf}{ft}$

$h := 8 \ ft$

$l := 12 \ ft$

$t := 9.625 \ in$

$A_n := 33 \ \frac{in^2}{ft}$

$b := 1 \ ft$

$f'_m := 1500 \ \frac{lbf}{in^2}$

$E_m := 750 \cdot f'_m = (1.125 \cdot 10^3) \ ksi$

$I_x := 635.3 \ \frac{(in)^4}{ft}$ (Taly, 2001)

$S := 117.8 \left(\frac{in^3}{ft}\right)$

$\phi := 0.6$

Calculate Wind Load

The loading from the 250mph wind is calculated using the procedure of ASCE 7-05 and special provisions from FEMA-361, Chapter 3, Section 5.1, Design Parameters. The coefficients provided by FEMA are:

$V := 250$ (Design Wind Speed)

$I := 1.0$ (Importance Factor)

Exposure Category: C

$K_d := 1.0$ (Directionality Factor)

$K_{zt} := 1.0$ (Topographic Effects)

$G := 0.85$ (Gust Effect Factor)

Enclosure Classification:
Partially Enclosed

$GC_{pi} := 0.55$ (Internal Pressure Coefficient)

Using these coefficients, the wind pressure, p, on the wall is calculated:

$K_z := 0.85$ (ASCE 7-05, Tbl. 6-3)

$C_p := -0.5$ (ASCE 7-05, Fig. 6-6)

$q_z := .00256 \cdot K_z \cdot K_{zt} \cdot K_d \cdot V^2 \cdot I \cdot \left(\frac{lbf}{ft^2}\right) = 136 \ \frac{lbf}{ft^2}$ (ASCE 7-05, 6.5.10)

$q := q_z$

$q_i := q_z$

$p := q \cdot G \cdot C_p - q_i \cdot (GC_{pi}) = -132.6 \ \frac{lbf}{ft^2}$ (ASCE 7-05, 6.5.12.2.1)

Now the ultimate wind load per foot-width of the masonry wall is determined:

$$w_u := \text{abs}(1.0 \cdot p \cdot b) = 132.6 \ \frac{lbf}{ft}$$ (FEMA-361, Load Combination 6)

This allows for a determination of the maximum moment felt by the wall per foot of width:

$$M_u := \frac{(w_u \cdot h^2)}{8} \cdot \left(\frac{1}{b}\right) = (1.061 \cdot 10^3) \ \frac{1}{ft} \cdot ft \cdot lbf$$

The required flexural strength is then found by dividng this maximum moment by the reduction factor of 0.6:

$$M_n := \frac{M_u}{0.6} = (2.122 \cdot 10^4) \ in \cdot \frac{lbf}{ft}$$

Calculate Available Existing Tensile Strength

$$f_r := 19 \ \frac{lbf}{in^2}$$ (ACI 530-08 Tbl. 2.2.3.2)

$$f_b := \frac{M_u}{S} - \frac{P_u}{A_n} = 98.97 \ \frac{lbf}{in^2}$$ (Ch. 3, Eq. G-1-1)

$$\phi f_r := 0.6 \cdot f_r = 11.4 \ \frac{lbf}{in^2}$$

$\phi f_r < f_b$ (Ch. 3, Eq. G-1-2)

Because the tensile strength provided by the mortar is less than that induced by the bending of the wall, additional flexural reinforcement is needed.

Determine Flexural Reinforcement

For this example, Aslan400 Carbon Fiber Laminate will be used. The fiber properties of this product are as follows:

$$f'_{fu} := 350 \ \frac{kip}{in^2} \qquad E_f := 19 \cdot 10^6 \ \frac{lbf}{in^2}$$

$$\varepsilon'_{fu} := 0.0187 \qquad t_f := 0.055 \ in$$

$$C_E := 0.85$$ (ACI 440.7R, Tbl. 8.1)

$$f_{fu} := C_E \cdot f'_{fu} = 297.5 \ \frac{kip}{in^2}$$ (ACI 440.7R, Eq. 8-3)

$\varepsilon_{fu} := C_E \cdot \varepsilon'_{fu} = 0.016$ (ACI 440.7R, Eq. 8-4)

In order to determine the amount of flexural reinforcement needed, the effective strain and stress for flexure controlled failure modes are calculated:

$\kappa_m := 0.45$ (ACI 440.7R, Eq. 8-8)

$\varepsilon_{fe} := \kappa_m \cdot \varepsilon'_{fu} = 0.008$

$C_E \cdot \varepsilon'_{fu} = 0.016$ (ACI 440.7R, Eq. 8-6)

$\varepsilon_{fe} < C_E \cdot \varepsilon'_{fu}$

$f_{fe} := \varepsilon_{fe} \cdot E_f = 159.885 \ \frac{kip}{in^2}$ (ACI 440.7R, Eq. 8-7)

Assuming the masonry crushing failure mode allows for taking the following values for the equivalent stres block:

$\gamma := 0.80$ (Ch. 3, Eq. G-1-3)

$\beta_1 := 0.80$ (Ch. 3, Eq. G-1-4)

Next, the neutral axis depth is solved for iteratevely such that the compressive strain in masonry exceeds maximum usable compressive strain of .0025. This will ensure that masonry crushing is the dominant failure mode.

$\varepsilon_{mu} := .0025$

Try: $c := 2.2 \ in$

$\varepsilon_m := \varepsilon_{fe} \cdot \left(\frac{c}{t - c} \right) = 0.0025$ (ACI 440.7R, Eq. 9-3)

With the neutral axis at 2.2in, the strain in the masonry is equal to the maximum usable masonry strain; hence, the balanced reinforcement condition occurs when the neutral axis is at a depth of 2.2in. Now that this neutral axis depth has been determined, it can be used to find the minimum area of reinforcement required to achieve this balanced condition. The minimum area of reinforcement per foot of width is:

$A_{f\_req} := \frac{\left(\gamma \cdot f'_m \cdot \beta_1 \cdot c - P_u \right)}{f_{fe}} = 0.157 \ \frac{1}{ft} \cdot in^2$ (ACI 440.7R, 13.1, Eq. a)

The total width of FRP reinforcement per widht is found by dividing this area by the thickness of the fiber:

$$b_{f\_req} := \frac{A_{f\_req}}{t_f} = 2.848 \ \frac{1}{ft} \cdot in$$

Therefore a single layer of 4in CFRP straps spaced at 12 in. on center should be used to reinforce both sides of the masonry wall.

$$b_f := 4 \ in \qquad d := t + t_f = 9.68 \ in$$

$$A_f := \frac{b_f \cdot t_f}{b} = 0.22 \ \frac{1}{ft} \cdot in^2 \qquad s := 12 \ in$$

Now that the an initial FRP layout has been determined, it must be checked to ensure that the spacing of the FRP strips is less than what is required by ACI 440.7R:

$$s_{max} := 3 \cdot t + b_f = 32.875 \ in \qquad \text{(ACI 440.7R, 11.3.1)}$$

Additionally, the area of reinforcement is checked to see that it is less than two times the balanced condition. This ensures that the failure mode remains masonry crushing, and that no ineffecient use of fiber occurs.

$$A_f \leq 2 \cdot A_{f\_req} = 1$$

Alternatively, because the masonry crushing failure mode is assumed, the required area of reinforcement can be determined directly from the balanced reinforcement ratio

$$\rho_{fb} := \frac{f'_m}{f_{fe}} \left(\gamma \cdot \beta_1 \cdot \left(\frac{\varepsilon_{mu}}{\varepsilon_{mu} + \varepsilon_{fe}} \right) - \frac{P_u \cdot b}{b \cdot t \cdot f'_m} \right) = 0.001 \qquad \text{(Ch. 3, Eq. G-1-6)}$$

$$A_{f\_req} := \rho_{fb} \cdot b \cdot t = 0.157 \ in^2 \qquad \text{(Ch. 3, Eq. G-1-5)}$$

This can then be used to find the location of the neutral axis by equating stresses. Rearranging Eq. 7 and accounting for Axial Loading gives:

$$c := \frac{A_{f\_req} \cdot f_{fe} + P_u \cdot b}{\gamma \cdot f'_m \cdot \beta_1 \cdot b} = 2.205\ in$$ (Ch. 3, Eq. G-1-7)

As expected, this matches the location of the neutral axis found using the iterative approach. Finally, we check to ensure that the required nominal flexural strength is achieved. This can be accomplished by considering moment equilibrium relative to center of compression of the masonry or FRP reinforcement, in this case, the stress in the masonry is considered:

$$M_{nc} := (\gamma \cdot f'_m) \cdot (\beta_1 \cdot c) \cdot b \cdot \left(d - \frac{\beta_1 \cdot c}{2}\right) + P_u \cdot \left(\frac{t}{2} - \frac{\beta_1 \cdot c}{2}\right) \cdot b = (1.872 \cdot 10^4)\ lbf \cdot ft$$

$$\phi \cdot M_{nc} = (1.123 \cdot 10^4)\ lbf \cdot ft$$

$$\phi \cdot M_{nc} \geq M_u \cdot b = 1$$

Determine Impact Strength Reinforcement

$m_w := 15\ lbm$ Wood Properties (Subalpine Fur)

$g = 32.174\ \frac{ft}{s^2}$ $E_w := 1.29 \cdot 10^3\ ksi$

$v_0 := 100\ mph = 146.667\ \frac{ft}{s}$ $v_w := 0.45$

$T_i := (1.5)\ ms = 0.0015\ s$

$$F_{impact} := \frac{2\ (m_w)\ (v_0)}{T_i} = 91.171\ kip$$ (Ch. 3, Eq. G-2-2)

$$K := \left(\frac{5\ in^{\frac{1}{2}}}{3}\right) \cdot \left(\frac{\left(1 - v_w^{\ 2}\right)}{E_w} + \frac{1}{E_m}\right)^{-1} = (1.215 \cdot 10^9)\ \frac{kg}{m^{\frac{1}{2}} \cdot s^2}$$ (Ch. 3, Eq. G-2-4)

The first step is to determine the flexural rigidity of FRP reinforced wall per unit width by considering the contribution of both the masonry and the added FRP reinforcement:

$$D := E_m \cdot (I_x) + E_f \cdot \frac{\left(b_f \cdot t_f \cdot t^2\right)}{4 \cdot b} = (8.115 \cdot 10^5)\ \frac{1}{ft} \cdot kip \cdot in^2$$

This leads to a determination of the equivalent bending stiffness of the wall, which is taken as a thin plate:

$$w_{max} := 0.02304 \cdot F_{impact} \cdot l \cdot \frac{h}{D} = 0.429\ in$$

$$k_{eq} := \frac{F_{impact}}{w_{max}} = \left(2.548 \cdot 10^3\right)\ \frac{kip}{ft} \qquad \text{(Ch. 3, Eq. G-2-5)}$$

The nominal impact force can then be calculated iteratively by choosing a nominal impact force in an attempt to equate both sides of Ch.3, Eq. G-2-3:

Choose Fn: $F_n := 139.8\ kip$

$$LHS := \left(\frac{1}{2}\right) \cdot m_w \cdot {v_0}^2 = 5.014\ kip \cdot ft \qquad \text{(Ch. 3, Eq. G-2-3)}$$

$$RHS := \left(\frac{1}{2}\right) \cdot \left(\frac{{F_n}^2}{k_{eq}}\right) + \left(\frac{2}{5}\right) \cdot \frac{\left({F_n}^{\frac{5}{3}}\right)}{K^{\frac{2}{3}}} = 5.009\ kip \cdot ft$$

$$\phi := 0.80$$

$$\phi \cdot F_n = 111.84\ kip$$

$$F_{impact} = 91.171\ kip$$

$$\phi \cdot F_n \geq F_{impact} = 1 \qquad \text{(Ch. 3, Eq. G-2-1)}$$

The impact resistance criterion is satisfied, therefore no further vertical reinforcement shall be added. However, in order to satisfy Section 3.2, equal horizontal reinforcement will be added to create an orthogonal grid. Therefore, the final reinforcement layout is a singel layer of 4in. CFRP strips spaced at 12in on center on both sides of the wall, running in horizontal and vertical directions. This layout is diagramed in figure 4.2 below.

Aslan 400 Mechanical Properties – Tensile, Modulus & Strain

Dimensions				Nominal Area		Guaranteed Tensile Strength		Ultimate Tensile Load		Tensile Modulus of Elasticity		Ultimate Strain
Width -in	Width - mm	Thickness - in	Thickness - mm	mm^2	in^2	MPa	ksi	kN	kips	GPa	psi 10^6	%
2	50	0.055	1.4	70	0.1102	2400	350	168	38.57	131	19	1.87%
4	100	0.055	1.4	140	0.2204	2400	350	336	77.14	131	19	1.87%

Hughes Brothers reserves the right to make improvements in the product and/or process which may result in benefits or changes to some physical-mechanical characteristics. The data contained herein is considered representative of current production and is believed to be reliable and to represent the best available characterization of the product as of July 2011. Tensile tests per ASTM D3039.

Figure 4.1Mechanical Properties of Aslan400 Carbon Fiber Reinforced Polymer

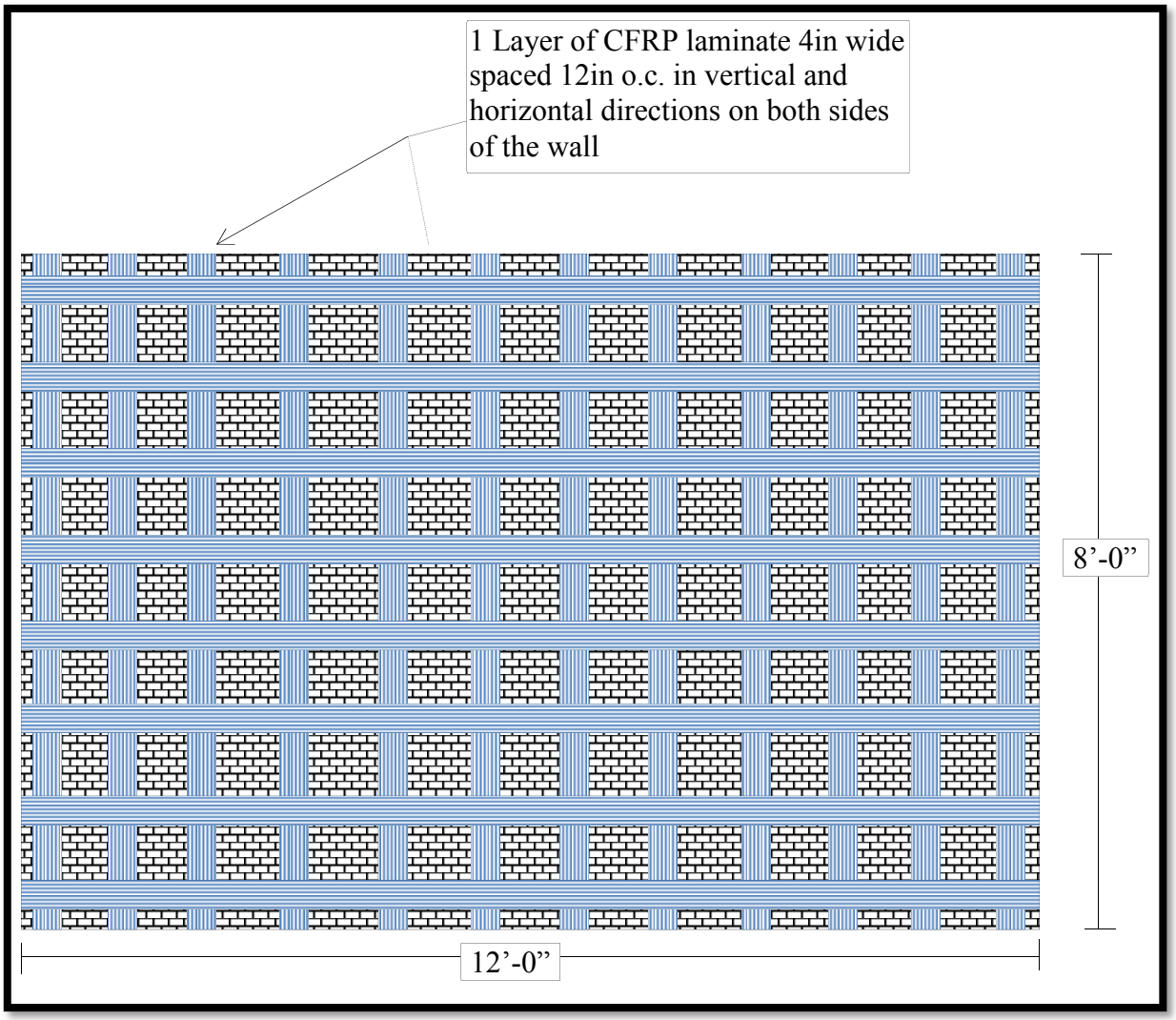

Figure 4.2 Recommended Reinforcement Layout for Design Example

The reinforcement resulting from this example illustrates some important points. First, even un-grouted, unreinforced masonry is capable of being reinforced to resist lateral and impact loading using FRP. This indicates the broader applicability for of this design procedure for under-reinforced masonry or concrete walls. Second, the amount of reinforcement required is reasonable and can easily be achieved using only a single layer of FRP reinforcement. This is significant because the design guidelines were developed using conservative estimates and assumptions and are intended to be an upper-bound for reinforcement to be later verified using a

full-scale experimental program. Last, it shows that by only slightly exceeding the balanced reinforcement condition, in this case $\rho=1.4\rho_{fb}$, adequate impact resistance strength can also be achieved. This verifies the experimental findings of Schmidt and Cheng (2009), and shows that the two FEMA-361 Tornado Safe Room design requirements can be easily integrated.

This design example shows that the guidelines developed have relevant, practical design applications. This fills the gap separating theoretical FRP application with the real world design guidelines presented to preserve the structural integrity of masonry buildings during a Tornado.

4.2 Limitations

As stated above, several assumptions are made which make the design equations, especially when designing for impact resistance, conservative. Particularly, it is assumed that the kinetic energy in the missile is equal to the energy stored in the wall after impact, when in reality; a large amount of energy is lost to vibration, heat, and deformation of the wooden missile. Because of the likely deformation of the timber during impact, the method proposed for determining force leads to an overestimation; however, due to field observations which indicate that such missiles remain sufficiently hard after impact, the approach used is within reason (Kennedy 1976). Neglecting this energy loss, the actual force experienced by the masonry will be much lower than what is assumed, providing a conservative estimate for the nominal impact strength F_n of the masonry. Indeed, little is known about the behavior of FRP reinforced masonry under high velocity impacts, and this lack of knowledge represents a major weakness of this study.

Additionally, the scope of recommendations is very narrow and considers only the wall of the Safe Room, independent of other structural elements. Without consideration of the rest of the structure and how the walls are connected with the roof, foundations, and other portions of the

building envelope, it is difficult to obtain a comprehensive understanding of how FRP reinforcement affects the global Safe Room design. Finally, it is claimed that the design guidelines presented in Chpater 3 allow for an engineer to retrofit a masonry wall so that it complies with the requirements of a FEMA Tornado Safe Room. While this may be true, FEMA-361 dictates that all safe room wall assemblies must pass debris impact-resistance testing as per the Test Method for Impact and Pressure Testing in Chapter 8 of ICC-500.

4.3 Future Research

The first area in which more research should be conducted is to better understand tornado behavior, especially the behavior of tornadic winds. Currently, little is understood about the nature of tornadic winds, and this uncertainty increases as one moves closer to the vortex where violent and complex rotational winds dominate.

Additionally, all of the evidence and assumptions made about the dynamic response of the FRP strengthened masonry come from two correlated studies. An additional full-scale experiment should be performed to observe the behavior of masonry reinforced with Fiber Reinforced Polymer. In order to fill the gaps presented in the findings of this thesis, experimental setup and test procedures should include:

- Construction of full-scale, single wythe masonry walls of 8in, 10in, and 12in units
- Reinforcing patterns of vertical strips, orthogonal and diagonal grids, and continuous woven and unidirectional sheets
- Testing should be firing of 15lb 2x4 wood timber at 100mph
- Response of wall should be recorded including deflection, perforation, cracking, and force on impact

- Determination of minimum requirement for FRP reinforcement of masonry equivalent to typical steel reinforcement as per FEMA-361, Chapter 7, Section 3.4, Impact Resistance of Concrete Masonry Units
- Impact testing should also be performed in accordance with provisions of Chapter 8 of ICC-500, Test Method for Impact and Pressure Testing

Such an experimental setup would provide much needed information as to the behavior of FRP reinforced masonry subject to high velocity impacts. Simultaneously, minimum standards for using FRP to provide impact resistance for Safe Shelters could be established, and the design equations in this document could be verified as reasonable upper-bounds for reinforcement.

Chapter 5 Conclusion

In the last half of the 20th Century, Tornados claimed more than 5000 lives, left 93,000 injured, and were responsible for an average of 57% of all insured catastrophic losses in the United States (FEMA P-361 2008). While the violent rotating winds and unpredictable damage paths of a tornado may seem like random acts of nature, the type of structure one finds demolished in its wake is far from arbitrary. Rigid behavior, a lack of axial compression, and unreliable tensile strength combine to make unreinforced masonry walls the most susceptible to damage in a tornado, and represent the greatest threat to human life and safety of all construction materials under similar loads (Mehta 1984). Even more alarming, communities designate URM gymnasiums, cafeterias, and bathrooms as storm shelters and assembly areas, ignorant to their inherent, hazardous structural behavior.

The goal of this thesis was to bring light to this deadly occurrence and provide ways to mitigate such a costly engineering oversight. After discussing the underlying reasons behind URM's poor performance in extreme wind events determined by both field studies and experimental investigations, a summary of research was presented to determine whether Fiber Reinforced Polymer composites could be used to retrofit URM walls to provide them with the strength needed to be considered for use in Tornado Safe Rooms, as specified by the leading U.S. design guide for storm shelters, FEMA-361. Using anchorage or surface preparation to ensure development of adequate bond strength, application of FRP is found to significantly increase the flexural strength of URM (Tan and Patoary 2004). It is found that published design guides on the FRP strengthening of URM walls can be successfully applied to fulfill the lateral load resistance criteria portion of FEMA-361's Safe Room Design Criteria.

Research is also beginning to investigate how FRP reinforcement affects the response of masonry under dynamic impact loads. Though this research is in its infancy, current evidence suggests that by providing enough FRP reinforcement to ensure masonry crushing as the failure mode FRP can also greatly improve CMUs impact resistance with some variation based on fiber layout, provided adequate bond strength is achieved (Schmidt and Cheng 2009).

All of these findings are summarized in a design guide that represents a first attempt at providing engineers with straight-forward way to use FRP to retrofit URM walls to satisfy the Tornado Safe Room requirements of FEMA-361. The qualities of Fiber Reinforced Polymers make this method for URM reinforcement a much more attractive alternative to conventional steel reinforcement which requires a significant amount of time, monetary investment, and disruption in serviceability of the structure.

These contributions are a promising step in the development of structural applications of FRP. Considering the loss of more than 600 lives and $25 billion in insured property due to tornadoes and thunderstorms in 2011, this represents the possibility of saving thousands of lives and millions of dollars in structural rehabilitation and insurance losses (Munich RE 2012). However, the design equations make several assumptions which overestimate the maximum impact force felt by the FRP strengthened walls under high velocity impact. The inexactness of these design equations highlights the future opportunities for investigation of FRP strengthening of URM walls, with specific attention given to their use to improve the impact resistance of masonry walls subject to high velocity impacts typical of a tornado. It is recommended that future experiments comply with the testing procedures outlined in ICC-500, and used by FEMA to verify a structural materials resiliency against high velocity impact. Such experiments could

greatly enhance the applicability of the findings of this investigation and help repair a devastating failure in U.S. building infrastructure.

References

ACI 440.7R-10. *Guide for the Design and Construction of Externally Bonded Fiber-Reinforced Polymer Systems for Strengthening Unreinforced Masonry Systems.* American Concrete Institute, 2010.

ACI 530-08. *Building Code Requirements for Masonry Structures.* American Concrete Institute, 2007.

Albert, Michael L., Alaa E. Elwi, and J.J. Roger Cheng. "Strengthening of Unreinforced Masonry Walls Using FRPs." *Journal of Composites for Construction*, May 2001: 76-84.

ASCE 7-05. *Minimum Design Loads for Buildings and Other Structures.* Reston: American Society of Civil Engineers, 2005.

Associated Press. *Damage from Joplin, Mo., tornado: $2.8 billion.* May 20, 2012. http://www.sfgate.com/nation/article/Damage-from-Joplin-Mo-tornado-2-8-billion-3571524.php.

Camli, Umit Serdar, and Baris Binici. "Strength of Carbon Fiber Reinforced Polymers Bonded to Concrete and Masonry." *Construction Building Materials* (Elsevier Ltd.) 21 (2007): 1431-1445.

Cheng, Lijuan, and Ashley M. McComb. "Unreinforced Concrete Masonry Walls Strengthened with CFRP Sheets and Strips under Pendulum Impact." *Journal of Composites for Construction* (ASCE), 2010: 775-783.

Coulbourne, William L., E. Scott Tezak, and Therese P. McAllister. "Design Guidelines for Community Shelters for Extreme Wind Events." *Journal of Architectural Engineering* (ASCE) 8 (June 2002): 69-77.

FEMA P-361. *Design and Construction Guidance for Community Safe Rooms.* U.S. Department of Homeland Security, Federal Emergency Management Agency, 2008.

Galati, N., E. Garbin, G. Tumialan, and A. Nanni. *Design Guidelines for Masonry Structures: Out of Plane Loads.* ACI, 2005.

Hamilton, H. R. , and C. W. Dolan. "Flexural Capacity of Glass FRP Strengthened Concrete Masonry Walls." *Journal of Composites for Construction* (ASCE) 5 (August 2001): 170-178.

Hamoush, Sameer A., Mark W. McGinley, Paul Mlakar, David Scott, and Kenneth Murray. "Out-of-Plane Strengthening of Masonry Walls with Reinforced Composites." *Journal of Composites fro Construction* (ASCE) 5 (August 2001): 139-145.

Kennedy, R.P. "A Review of Procedures for the Analysis and Design of Concrete Structures to Resist Missile Impact Effects." *Nuclear Engineering and Design*, 1976: 183-203.

McDonald, James R. "Impact Resistance of Common Building Materials to Tornado Missiles." *Journal of Wind Engineering and Industrial Aerodynamics* (Elsevier Science Publishers B.V.) 36 (1990): 717-724.

Mehta, Kishor C. "Wind Induced Damage Observations and Their Implications for Design Practice." *Engineering Structures* (Butterworth & Co.) 6 (October 1984): 242-247.

Munich RE. *2011 Natural Catastrophe Year in Review.* Munich Reinsurance America, Inc., 2012.

NOAA. "Monthly and Annual U.S. Tornado Summaries." *NOAA's National Weather Service Storm Prediction Center.* January 6, 2013. www.spc.noaa.gov/climo/online/monthly/newm.html.

Prevatt, David O., William Coulbourne, Andrew J. Graettinger, Shiling Pei, Rakesh Gupta, and David Grau. *Joplin, Missouri, Tornado of May 22, 2011.* Reston, Virginia: American Society of Civil Engineers, 2013.

Schmidt, Mason E., and Lijuan Cheng. "Impact Response of Externally Strengthened Unreinforced Masonry Walls Using CFRP." *Journal of Composites for Construction* (ASCE), July/August 2009: 252-261.

Sparks, Peter R., Henry Liu, and Herbert S. Saffir. "Wind Damage to Masonry Buildings." *Journal of Aerospace Engineering*, 1989: 186-198.

Taly, Narendra. *Design of Reinforced Masonry Structures.* New York: McGraw-Hill, 2001.

Tan, Kiang Hwee, and M. K. H. Patoary. "Strengthening of Masonry Walls against Out-of-Plane Loads Using Fiber-Reinforced Polymer Reinforcement." *Journal of Composites for Construction* (ASCE), January/February 2004: 79-87.

Triantafillou, Thanasis C. "Strengthening of Masonry Structures Using Epoxy-Bonded FRP Laminates." *Journal of Composites for Construction* (ASCE) 2 (May 1998): 96-204.

USGS. "Deaths from U.S. Earthquakes." *USGS Earthquake Hazards Program.* January 1, 2013. earthquake.usgs.gov/earthquakes/states/us_deaths.php.

Velazquez-Dimas, J. I., and M. R. Ehsani. "Modeling Out-of-Plane Behaviour of URM Walls Retrofitted with Fiber Composites." *Journal of Composites for Construction* (ASCE), November 2000: 172-181.

Appendix

Determination of Nominal Impact Strength

The nominal impact strength of a wall under a point impact is determined using the Hertzian Law of Contact (Schmidt and Cheng 2009). The maximum impact resistance of a wall F_{impact_max} is found by solving the following equation iteratively:

$$\frac{1}{2}m_1 v_0^2 = \left(\frac{1}{2}\right)\left(\frac{F_{impact\_max}^2}{k_{bs}}\right) + \left(\frac{2}{5}\right)\left(\frac{F_{impact\_max}^{\frac{5}{3}}}{K^{\frac{2}{3}}}\right)$$

Let $F_{impact\_max}=F_n$ (nominal impact strength)

To solve for the equivalent stiffness of the wall the first step is to find the specific flexural rigidity (bending stiffness) of the composite wall/frp system :

$$D_b = E_m I_m + E_f I_f$$

$$I_f = E_m I_m + b_f t\left(\frac{h}{2} + \frac{t}{2}\right)^2$$

Neglecting contribution of flange inertia about its own axis and thickness of FRP with respect total thickness:

$$I_f = \frac{b_f t h^2}{4}$$

$$I_m = \left(\frac{1}{12}\right) b h^3$$

Substituting these values into D and dividing by unit width b to find the specific flexural rigidity gives:

$$D = E_m(I_x) + E_f\left(\frac{b_f t h^2}{b \cdot 4}\right)$$

Where I_x=moment of inertia of masonry for a horizontal cross section per foot of width.

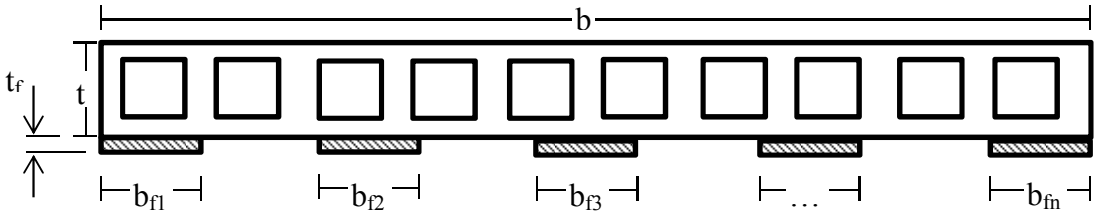

$$b_f = \frac{\sum_{i=1}^{n} b_{fi}}{b}$$

The equivalent bending stiffness is found considering the wall as a Timoshenko beam of unit width b such that:

$$k_{eq} = \frac{F_{impact}}{w_{max}}$$

Where

$$w_{max} = 0.02304 Plh/D$$

and l and h are the length and height of the wall.

K represents a constant based on the stiffness of the missile and impacted service calculated as:

$$K = (4/3)R_w^{1/2}\left[\frac{1-v_w^2}{E_w} + \frac{1}{E_m}\right]^{-1}$$

To solve one simply replaces R_w with the equivalent radius for a wood 2x4:

$$2in \cdot 4in = \pi \cdot R_w^2$$

$$R_w = \sqrt{\frac{8}{\pi}}$$

$$R_w = 1.6$$

Plugging back in for K and solving:

$$K = \frac{4\sqrt{1.6}}{3}\left[\frac{1-v_w^2}{E_w}+\frac{1}{E_m}\right]^{-\frac{1}{3}}$$

$$K = \frac{5}{3}\left[\frac{1-v_w^2}{E_w}+\frac{1}{E_m}\right]^{-1/3}$$

Therefore:

$$\frac{1}{2}m_1 v_0^2 = \left(\frac{1}{2}\right)\left(\frac{F_n^2}{k_{eq}}\right)+\left(\frac{2}{5}\right)\left(\frac{F_n^{\frac{5}{3}}}{K^{\frac{2}{3}}}\right)$$

where

$$K = \frac{5in^{\frac{1}{2}}}{3}\left[\frac{1-v_w^2}{E_w}+\frac{1}{E_m}\right]^{-1/3}$$

and

$$k_{eq} = \frac{F_{impact}}{w_{max}} = \frac{1}{(0.02304)\frac{lh}{d}}$$